

การสร้างแบบจำลองเชิงโมเลกุลและการจำลองพลวัตเชิงโมเลกุลของโดเมนรับรู้ความต่างศักย์  
ของโซเดียมแชนแนลในสถานะกระตุ้นและสถานะพัก

นางสาววรรณฤดี วรรณภักดี

วิทยานิพนธ์นี้เป็นส่วนหนึ่งของการศึกษาตามหลักสูตรปริญญาวิทยาศาสตรมหาบัณฑิต  
สาขาวิชาเคมี ภาควิชาเคมี

คณะวิทยาศาสตร์ จุฬาลงกรณ์มหาวิทยาลัย

ปีการศึกษา 2555

ลิขสิทธิ์ของจุฬาลงกรณ์มหาวิทยาลัย

บทคัดย่อและแฟ้มข้อมูลฉบับเต็มของวิทยานิพนธ์ตั้งแต่ปีการศึกษา 2554 ที่ให้บริการในคลังปัญญาจุฬาฯ (CUIR)

เป็นแฟ้มข้อมูลของนิสิตเจ้าของวิทยานิพนธ์ที่ส่งผ่านทางบัณฑิตวิทยาลัย

The abstract and full text of theses from the academic year 2011 in Chulalongkorn University Intellectual Repository(CUIR)  
are the thesis authors' files submitted through the Graduate School.

MOLECULAR MODELING AND MOLECULAR DYNAMICS SIMULATION  
OF VOLTAGE SENSOR DOMAIN OF SODIUM CHANNEL  
IN ACTIVATED AND RESTING STATES

Miss Wannaruedee Wannapukdee

A Thesis Submitted in Partial Fulfillment of the Requirements  
for the Degree of Master of Science Program in Chemistry

Department of Chemistry

Faculty of Science

Chulalongkorn University

Academic Year 2012

Copyright of Chulalongkorn University

Thesis Title                                    MOLECULAR MODELING AND MOLECULAR  
DYNAMICS SIMULATION OF VOLTAGE SENSOR  
DOMAIN OF SODIUM CHANNEL IN ACTIVATED  
AND RESTING STATES  
By    Miss Wannaruedee Wannapukdee  
Field of Study                                Chemistry  
Thesis Advisor                               Associate Professor Pornthep Sompornpisut, Ph.D.

---

Accepted by the Faculty of Science, Chulalongkorn University in Partial  
Fulfillment of the Requirements for the Master's Degree

..... Dean of the Faculty of Science  
(Professor Supot Hannongbua, Dr.rer.nat.)

#### THESIS COMMITTEE

..... Chairman  
(Assistant Professor Warinthorn Chavasiri, Ph.D.)

..... Thesis Advisor  
(Associate Professor Pornthep Sompornpisut, Ph.D.)

..... Examiner  
(Associate Professor Sirirat Kokpol, Ph.D.)

..... External Examiner  
(Arthorn Loisruangsin, Ph.D.)

วรรณฤดี วรรณภักดี : การสร้างแบบจำลองเชิงโมเลกุลและการจำลองพลวัตเชิงโมเลกุล  
ของโดเมนรับรู้ความต่างศักย์ของโซเดียมแชนแนลในสถานะกระตุ้นและสถานะพัก  
(MOLECULAR MODELING AND MOLECULAR DYNAMICS SIMULATION OF  
VOLTAGE SENSOR DOMAIN OF SODIUM CHANNEL IN ACTIVATED AND  
RESTING STATES) อ.ที่ปรึกษาวิทยานิพนธ์หลัก : รศ.ดร.พรเทพ สมพรพิสุทธิ, 62 หน้า

โวลเทจเกตโซเดียม แชนแนล ( $\text{Na}_v$ ) เป็นเมมเบรนโปรตีนที่ควบคุมการไหล  
ของโซเดียมไอออนผ่านเมมเบรนทั้งเซลล์ยูคาริโอตและโปรคาริโอต มีบทบาทต่อการ  
สร้างและส่งสัญญาณของ ศักย์ไฟฟ้าในเซลล์ที่ถูกกระตุ้น ได้มีการพัฒนาแบบจำลอง  
โครงสร้างของโดเมนรับรู้ ศักย์ไฟฟ้า (VSD) ของโซเดียมแชนแนลในแบคทีเรีย *Bacillus*  
*halodurans* (NaChBac) ในสถานะกระตุ้นหรือ “อ็อป” ด้วยการวิเคราะ การจำลอง  
พลวัตเชิงโมเลกุล โดยใช้ข้อมูลไซลเวนท์แอกเซสซิบิลิตีที่ได้จากกา รทดลอง ใน  
การศึกษานี้ ได้สร้างคอนฟอร์เมชันของสถานะพักหรือ “ดาวน” โดยอนุมานจากข้อมูล  
ทางชีวฟิสิกส์และชีวเคมี ได้สำรวจ โครงสร้าง และพลวัตของอ็อปและดาวนคอนฟอร์เม  
ชันโดยใช้การจำลองพลวัตเชิงโมเลกุลในฟอสโฟลิพิดไบเลเยอร์ จากผลการจำลองพบว่า  
โครงสร้างส่วนทรานส์ เมมเบรนของสถานะอ็อปเสถียรกว่าสถานะดาวน พบการ  
แลกเปลี่ยนของคู่ประจุตรงข้ามระหว่างอาร์จินีนบน S4 กับกรดอะมิโนประจุลบบน S1,  
S2 และ S3 รวมทั้งรอยแยกที่น้ำเข้าไปได้ภายในโพรงของ VSD มีขนาดเพิ่มขึ้น ซึ่ง  
สนับสนุนข้อมูลที่พบเห็นจากการทดลอง แม้ว่าการแปลผลของการศึกษานี้เป็ นไปตาม  
แบบจำลองที่พัฒนาจากโครงสร้างผลึกของโปแตสเซียม แชนแนล ผลการศึกษานี้ให้  
ข้อมูลที่เป็นประโยชน์สำหรับการเคลื่อนที่ของส่วนรับรู้ ศักย์ไฟฟ้าภายใน ด้บริบทของ  
กลไกการหมุนควงของเกลียวเฮลิคซ์

ภาควิชา.....เคมี.....

ลายมือชื่อนิสิต.....

สาขาวิชา.....เคมี.....

ลายมือชื่อ อ.ที่ปรึกษาวิทยานิพนธ์หลัก.....

ปีการศึกษา.....2555.....

## 5372462823: MAJOR CHEMISTRY

KEYWORDS: NaChBac, Sodium channel, Voltage-sensor domain, Molecular dynamics simulations, Electrostatic solvation free energy

WANNARUEDEE WANNAPUKDEE: MOLECULAR MODELING AND MOLECULAR DYNAMICS SIMULATION OF VOLTAGE SENSOR DOMAIN OF SODIUM CHANNEL IN ACTIVATED AND RESTING STATES. ADVISOR: ASSOC. PROF. PORNTHEP SOMPORNPISTUT, Ph.D., 62 pp.

Voltage-gated sodium ( $\text{Na}_v$ ) channels are membrane proteins that control the flux of sodium ions through membrane in both eukaryotic and prokaryotic cells. They are responsible for generation and propagation of electrical potential in excitable cells. A structure model of the voltage-sensor domain (VSD) of a *Bacillus halodurans* Na channel (NaChBac) in the activated or “Up” state was previously developed using Restrained Molecular Dynamics with experimental solvent accessibility data. In this study the putative resting or “Down” conformation was built based on biophysical and biochemical data. Structure and dynamics of both Up and Down conformations were investigated by MD simulations in phospholipid bilayer. From the MD results, the transmembrane structure of the Up state is more stable than that of the Down state. A counter charge exchange between the S4 arginines and the negatively charge residues in S1, S2 and S3 and the increase of water-filled crevice of the VSD cavity supported the observation from experimental studies. Although, all the interpretations of the study are relied on the model developed based on the crystal structure of  $\text{K}_v$  channels, the results of this study provide useful information for a general motion of the voltage sensing segment in a context of helical screw mechanism.

Department : \_\_\_\_\_ Chemistry \_\_\_\_\_

Student's Signature : \_\_\_\_\_

Field of Study : \_\_\_\_\_ Chemistry \_\_\_\_\_

Advisor's Signature : \_\_\_\_\_

Academic Year : \_\_\_\_\_ 2012 \_\_\_\_\_

## ACKNOWLEDGEMENTS

I wish to express my deep gratitude to a number of people who giving me the guidance, help and support to reach my goal of this thesis.

First of all, I would like to thank my supervisor, Associate Professor Dr. Pornthep Sompornpisut for his suggestion, continuous support kindness, knowledge about computational chemistry and encouragement thought the years of my study. I also thank my committee, Assistant Professor Dr. Warinthorn Chavasiri, Associate Professor Dr. Sirirat Kokpol and Dr. Arthorn Loiruangsinn for their discussion and guidance.

I would like to express my gratitude to the computational chemistry unit cell (CCUC) at Department of Chemistry, Faculty of Science, Chulalongkorn University for providing the facilities throughout the course of study.

My special thank to my family, for their loves, continuous sacrifice and moral support throughout the education course. On the other hand, I would like to thank Miss Weeraya Singcanipa, Miss Sunan Kitjaruwankul, Miss Sunit Fukang, Miss Pattama Wapeesittipan, Miss Kanokporn Petnapapun, Mr. Kanon Sujaree, Mr. Jarewat Jakmune and Mr. Chirayut Supunyabut for their friendships and help me for graduate research.

Finally, I would like to thank the National Research University Project of CHE, Ratchadaphiseksomphot Endowment Fund (HR1155A) and the Thai Government Stimulus Package 2 (TKK2555) for their support.

# CONTENTS

	<b>Page</b>
<b>ABSTRACT (THAI)</b> .....	iv
<b>ABSTRACT (ENGLISH)</b> .....	v
<b>ACKNOWLEDGEMENTS</b> .....	vi
<b>CONTENTS</b> .....	vii
<b>LIST OF TABLES</b> .....	ix
<b>LIST OF FIGURES</b> .....	x
<b>LIST OF PROGRAMMING</b> .....	xiii
<b>LIST OF ABBREVIATIONS</b> .....	xiv
<b>CHAPTER I INTRODUCTION</b> .....	1
<b>1.1 Ion channels</b> .....	1
<b>1.2 Voltage – gated ion channels</b> .....	3
<b>1.3 Na<sub>v</sub> channel structure</b> .....	6
1.3.1 General molecular structure and transmembrane topology.....	6
1.3.2 The Na <sub>v</sub> family.....	7
1.3.3 Role in action potential.....	8
<b>1.4 Literature reviews</b> .....	9
1.4.1 Discovery of the first Na <sub>v</sub> channels.....	9
1.4.2 Molecular basis and transmembrane topology of NaChBac.....	9
1.4.3 Voltage sensor domain: the functional independent domain.....	10
<b>1.5 Voltage sensing mechanism: how does the voltage sensor move?</b>	11
<b>1.6 The objectives of this research</b> .....	13
<b>CHAPTER II MATERIALS AND METHODS</b> .....	14
<b>2.1 Materials</b> .....	14
2.1.1 Hardware.....	14
2.1.2 Software.....	14
<b>2.2 Methods</b> .....	15
2.2.1 Modeling of NaChBac-VSD in the up state.....	15

	<b>Page</b>
2.2.2 Modeling of NaChBac-VSD in the intermediate and down - state.....	17
2.2.3 Calculating electrostatic solvation free energy.....	17
2.2.4 Molecular dynamics simulation.....	19
2.2.5 Analysis of MD trajectory.....	21
<b>CHAPTER III RESULTS AND DISCUSSION.....</b>	<b>22</b>
<b>3.1 Primary structure and sequence alignment of NaChBac-VSD...</b>	<b>22</b>
<b>3.2 Structure model in the activated state.....</b>	<b>23</b>
<b>3.3 Structure models in the down and intermediate states.....</b>	<b>26</b>
<b>3.4 Electrostatic solvation free-energy by Poisson – Boltzmaan solvent continuum method.....</b>	<b>28</b>
3.4.1 Electrostatic solvation energy of NaChBac-VSD as a function of $\epsilon$ and membrane thickness.....	28
3.4.2 Solvation energies of $K_v$ and $Na_v$ voltage sensors.....	29
3.4.3 Electrostatic solvation energy of activated, intermediate and open models.....	31
<b>3.5 MD simulation of up, intermediate and down models.....</b>	<b>32</b>
3.5.1 Structure and dynamic fluctuation.....	32
3.5.2 Evidence of structure instability.....	35
3.5.3 Salt bridge interactions.....	39
3.5.4 Water-filled crevices in the VSD core.....	42
3.5.5 Proposed transition model.....	46
<b>CHAPTER IV CONCLISIONS.....</b>	<b>47</b>
<b>REFERENCES.....</b>	<b>49</b>
<b>APPENDIX.....</b>	<b>54</b>
<b>VITAE.....</b>	<b>62</b>



**LIST OF TABLES**

<b>Table</b>		<b>Page</b>
3.1	Electrostatic solvation energies of NaChBac-VSD as a function of $\epsilon$ and membrane thickness ( $L_{\text{mem}}$ ).....	28
3.2	Electrostatic solvation energies of $K_v$ and $Na_v$ voltage sensors ( $\epsilon_{\text{protein}} = 4$ , $L_{\text{mem}} = 30 \text{ \AA}$ ).....	29
3.3	Electrostatic solvation energy of the S4 arginines.....	30
3.4	RMSD of the individual VSD segments averaged from the last 10-ns MD trajectories.....	33
3.5	The average RMSF for backbone atoms of transmembrane segments..	35

## LIST OF FIGURES

<b>Figure</b>		<b>Page</b>
1.1	Classification of ion channels based on external stimuli. From left to right: voltage-gated ion channels, ligand-gated (extracellular ligand) ion channels, ligand-gated (intracellular ligand) ion channels and mechanically gated ion channels.....	2
1.2	In nervous cells, the voltage – gated sodium channels generate and propagate of nerve impulse.....	3
1.3	The superfamily of ion channels are sodium channel, potassium channel and calcium channel. They are specific to sodium ions, potassium ions and calcium ions, respectively.....	4
1.4	The general structure of voltage – gated ion channels. Each domain is consisted of six transmembrane S1 – S6. The VSD (green) is a positively charged arginine on S4 at every third position. The PD (orange) form S5 - S6 helices that is the region for ions pass through to membrane. And c) when the changing membrane potential to depolarization state, the S4 helix moves outwardly the membrane and results to the PD open.....	5
1.5	The structure of Na <sub>v</sub> channels are a homotetramer that composed of four domain. Each monomer is consisted of the six transmembrane (S1 – S6).....	6
1.6	The voltage – gated sodium channels can be classified into four groups by location on human chromosome.....	7
1.7	The action potential of nervous cells .....	8
1.8	Transmembrane topology of NaChBac.....	10
1.9	The motion mechanisms of the S4 segment in VSD. From left to right, a) the helical – screw model, b) the transporter model and c) the paddle model.....	12

<b>Figure</b>	<b>Page</b>
2.1	Methodology flow chart for constructing structure model of NaChBac-VSD..... 16
2.2	Model systems used to compute electrostatic free energy of protein solvation. (A) The VSD is embedded in the membrane. The membrane region between the two blue planes is assigned a dielectric value $\epsilon_m = 2$ . Bulk water above and below the membrane is assigned a dielectric value of $\epsilon_w = 80$ . (B) The VSD in the bulk water ( $\epsilon_w = 80$ ) without the membrane. The protein solvation energy is calculated by $\Delta G_{elec} = \Delta G_A - \Delta G_B$ ..... 18
2.3	The membrane proteins system, Palmitoyl oleoyl phosphatidyl Cholines are membrane bilayer and TIP3P are force field parameter for water molecules..... 19
3.1	The sequence alignments of VSD – NaChBac are compared with Kv1.2 – 2.1, Kv1.2 and KvAP and the S4 helix consists of arginine or lysine at every third positions. The S1 – S3 helices have been a negatively charged residues that form salt – bridge interactions with the positively charged residue on S4..... 23
3.2	Structural model in the up state is shown in (A) cartoon model (B) surface model with electrostatic potential..... 24
3.3	Comparison of VSD structures: Na <sub>v</sub> versus K <sub>v</sub> ..... 24
3.4	Comparison of VSD structures: NaChBac (yellow) versus NavAb (red)..... 25
3.5	Structure models of the up, intermediate and down states of NaChBac-VSD..... 27
3.6	Per-residue contribution to the solvation energy (A) all residues of voltage sensor domain, (B) residues on the S4 segment and (C) 30
3.7	The relative electrostatic free energy of all five states are compared with the up state..... 31
3.8	Backbone RMSD with respect to the starting structure of all five

<b>Figure</b>		<b>Page</b>
	MD systems as a function of simulation time.....	32
3.9	RMSD of individual TM segment (S1-S4) of all five MD systems as a function of time.....	34
3.10	Backbone RMSF values as a function of residue number of NaChBac-VSD computed using the last 10-ns of simulations. The transmembrane regions are indicated by stripped background.....	36
3.11	Stability of secondary structure helices of the four TM segments as a function of simulation time calculated by DSSP. The each color mean : $\alpha$ -helix (red), stand in $\beta$ -sheet (blue), $\beta$ -bridge (yellow), $\beta$ -turn (black), coil (green), unassigned (white).....	38
3.12	The values of distances that represent key interactions in the four arginines of S4 of NaChBac-VSD. The distances are plotted on a color scale from blue (less than or equal to 2 Å) to red (greater than or equal to 8 Å).....	41
3.13	Density profile, comparing the distribution of water, lipids, and the four arginines in simulations of the up, intermediate and down states. The densities were averaged over the last 10 ns. ....	44
3.14	Water – filled crevices in the VSD core.....	45
3.15	The proposed transmittion of “up”, “int” and “down” states of NaChBac – VSD.....	46

**LIST OF PROGRAMMING**

<b>Script</b>		<b>Page</b>
A.1	Analysis script backbone RMSD.....	56
A.2	Analysis script RMSD of individual TM segment.....	57

## LIST OF ABBREVIATIONS

Na <sub>v</sub>	voltage-gated sodium channels
K <sub>v</sub>	voltage-gated potassium channels
Ca <sub>v</sub>	voltage-gated calcium channels
VSD	voltage sensor domain
PD	pore domain
S	segment
TM	transmembrane
NaChBac	sodium channels of the bacterium <i>Bacillus Halodurans</i>
CatSper	a mammalian putative voltage-gated cation channels of sperm
KvAP	voltage-dependent potassium channel from <i>Aeropyrum pernix</i>
Ci - VSP	<i>Ciona intestinalis</i> voltage-sensitive phosphatase
H <sub>v</sub>	voltage-sensitive proton channels
Å	angstrom
°	degree
IP	internet protocol
MD	molecular dynamics
PDB	protein data bank
PSF	protein structure file
VMD	visual molecular dynamics
APBS	adaptive Poisson-Boltzmann solver
PBE	Poisson-Boltzmann equation
PaDSAR	pseudoatom-driven solvent accessibility refinement
EPR	electron paramagnetic resonance
α	alpha
SDSL	Site-directed spin labeling
R	arginine acid
D	asplatic acid

E	glutamic acid
Q	glutamine acid
$\Delta G_{\text{elec}}$	electrostatic salvation free energy
$\Delta G_{\text{elec,membrane}}$	electrostatic salvation free energy of membrane
$\Delta G_{\text{elec,water}}$	electrostatic salvation free energy of membrane
$L_{\text{mem}}$	range of membrane bilayer thickness
$\epsilon_{\text{m}}$	dielectric constant of the membrane
$\epsilon_{\text{w}}$	dielectric constant of the water
$\epsilon_{\text{protein}}$	dielectric constant of the protein
POPC	palmitoyl oleoyl phosphatidyl cholines
LD	Langevin dynamics
ns	nanosecond
fs	femtosecond
ps	picosecond
RMSD	root-mean square deviation
RMSF	root-mean square fluctuation
3D	three dimentional
NavAb	voltage-gated sodium channel from the bacterium <i>Arcobacter butzleri</i>
Int	intermediate state
Down <sub>1</sub>	structural model type I of down state
Down <sub>2</sub>	structural model type II of down state
Down <sub>3</sub>	structural model type III of down state
kcal	kilocalorie
mol	mole
mV	milivolt
DSSP	database of secondary structure assignments of all protein
$\beta$	beta

# CHAPTER I

## INTRODUCTION

### 1.1 Ion Channels

Ion channels are proteins embedded in the membrane of biological cells. They can be found in all living cell. They play a fundamental role in physiological processes such as signal transduction, transmission and regulation of nerve impulse and muscle contraction etc [1]. Potassium and sodium ( $K^+$  and  $Na^+$ ) channels are the major ion channels of the nervous system [2]. The important function of these ion channels is to control the passage of the ions between the outside and the inside of the membrane in order to maintain the membrane potential for transmitting electrical or chemical signals along nerve cells [3].

There are many different types of ion channels which may be classified by different properties. Two most important features used for ion channel classification are the gating mechanism and the ion selectivity [4]. The selectivity of ion channels is related to ion types, specifically size and charge of the ions such as  $K^+$ ,  $Na^+$ ,  $Ca^{2+}$  and  $Cl^-$  channels [5]. Generally, there is a part of ion channels called “the gate”. The passage of ions is associated with the closing or opening of the gate of ion channels. Ion channels that are classified by the gating mechanisms can be defined on the basis of chemical and physical effects on the opening and closing of the pore [6], as shown in Figure 1.1.

Voltage-gated ion channels open and close in response to changes of membrane potential. An example of these ion channels is voltage-dependent potassium and sodium channels [7]. Ligand-gated channels have a receptor binding site recognized by specific ligands such acetylcholine, dopamine or serotonin etc. Upon the ligand binding, the channel is activated and undergoes conformational changes from the closed to the open state of the channels [8-9]. There are ion channels that can be activated by physical stimuli for instance, mechanosensitive ion channels. This channel is activated by sensing osmolytic stretch [10].



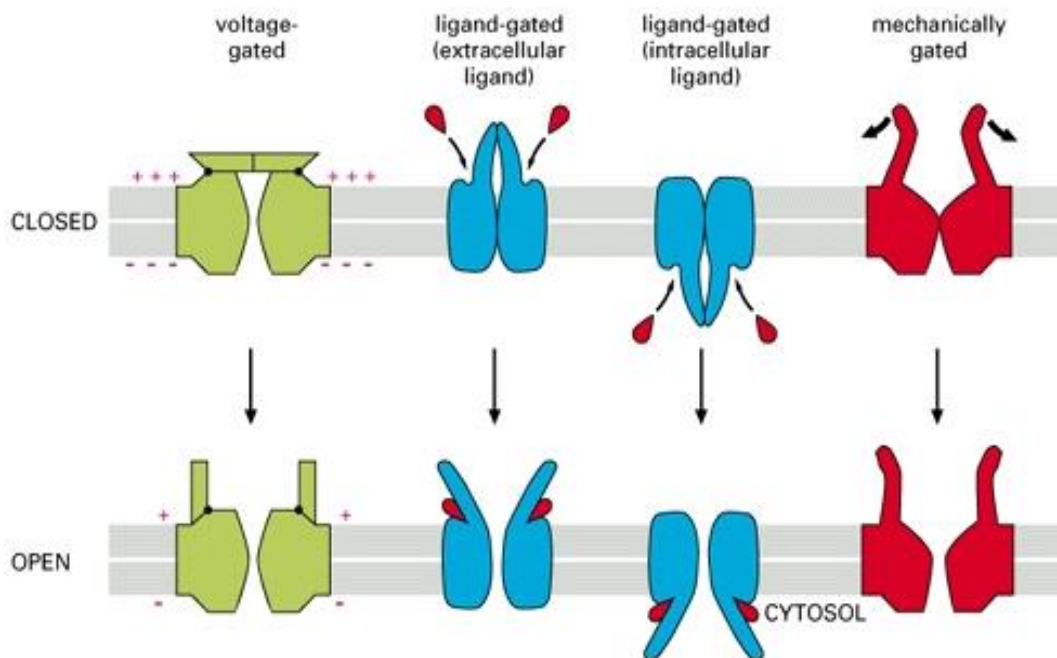


**Figure 1.1** Classification of ion channels based on external stimuli. From left to right: voltage-gated ion channels, ligand-gated (extracellular ligand) ion channels, ligand-gated (intracellular ligand) ion channels and mechanically gated ion channels [11].

There are many diseases associated with a malfunction of ion channels, for example prostate cancers, lung cancers, human cervical cancers, alzheimer's disease etc. The study of malfunctioning ion channels can provide useful information for pharmaceutical development and medical treatment [12].

## 1.2 Voltage-gated ion channels

Ion transmission occurs in the area of axons, of which the structure was covered by phospholipid bilayer. The axons have membrane proteins that act as a selective pore for specific ion passing across membrane bilayer. These membrane proteins called voltage-gated ion channels are activated by changes in electrical potential at the membrane [13]. Voltage-gated ion channels such as voltage-dependent potassium ( $K_v$ ) and sodium ( $Na_v$ ) channels are the most important ion channel in the class [14]. In neuron, they control ion diffusion across the membrane to generate and propagate of nerve impulse, as shown in Figure 1.2.

The superfamily of voltage-gated ion channels includes three major classes such as sodium channels, calcium channels and potassium channels [15]. These channels are typically a protein tetramer that forms a pore with ion permeation. The pore is specific to a particular passage of ions such as sodium ions, calcium ions and potassium ions, respectively as shown in Figure 1.3.

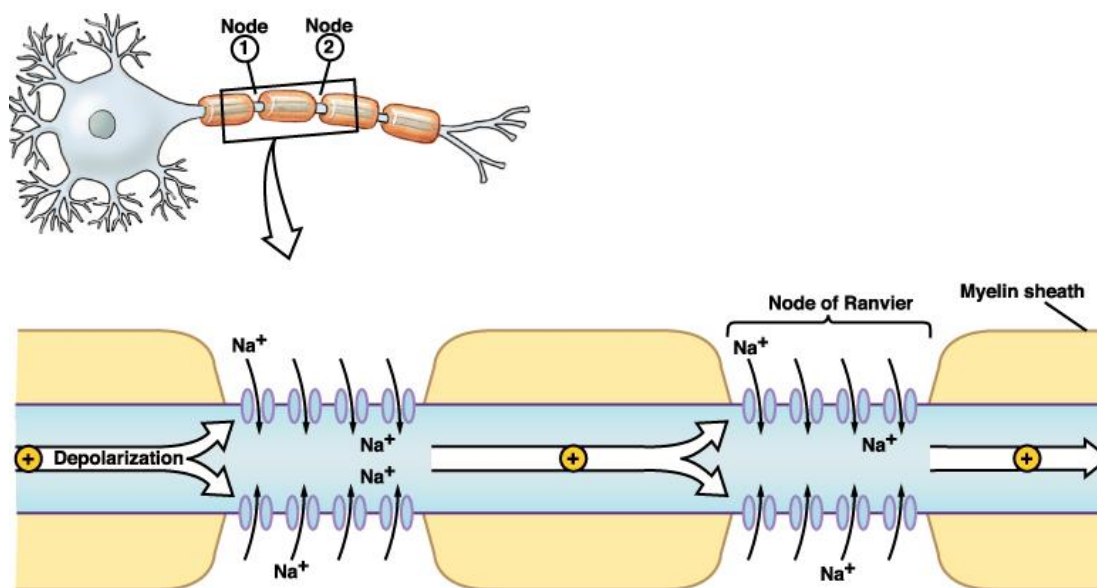


**Figure 1.2** In nervous cells, the voltage – gated sodium channels generate and propagate of nerve impulse [16].

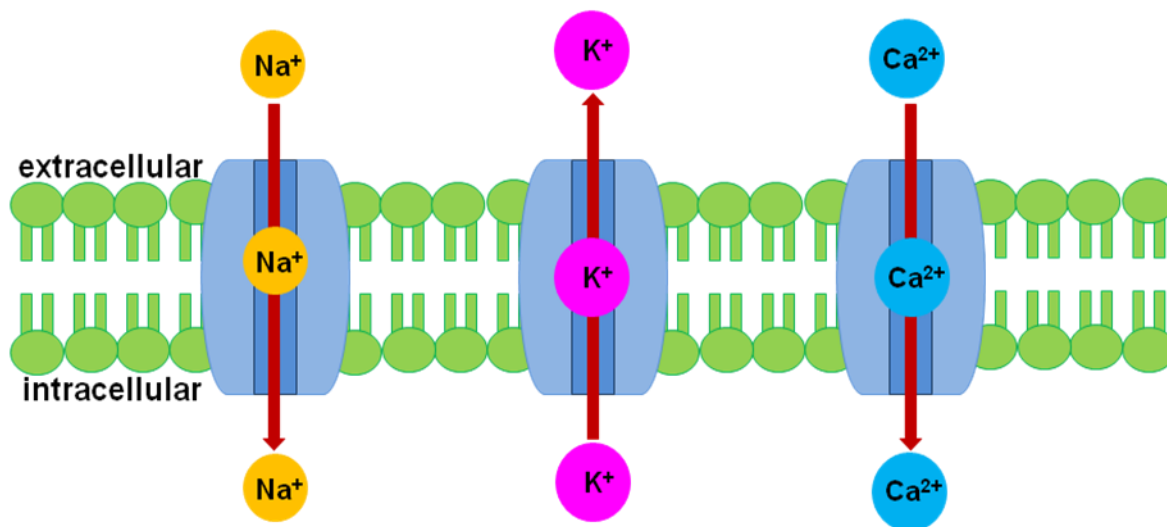


**Figure 1.3** The superfamily of ion channels are sodium channel, potassium channel and calcium channel. They are specific to sodium ions, potassium ions and calcium ions, respectively.

Voltage-gated ion channels typically form a hydrophilic hole, called pore which permeates for specific ions to pass through membrane. The pore formed by a multimeric assembly of transmembrane segments. They can be in the form of homo- or heterotetramer, depending upon types of the ion channels. Homotetrameric channels are less complicated for structural studies, and thus the most studied ion channels proteins are from bacteria or prokaryotic cells. Each monomer contains six transmembrane segments (S1-S6), each of which forms an  $\alpha$ -helix conformation. Amino acid composition and structural arrangement of voltage-gated ion channels has made two distinct functional domains in the protein that is called pore domain (PD) and voltage sensor domain (VSD) [14]. The PD allowing the passage of ions contains the last two segments, S5 and S6, whilst the VSD is formed by the first four segments, S1 to S4, as shown in Figure 1.4. The VSD do not perform a direct ion permeation function as in PD. The VSD detects and responds changes of membrane voltage by undergoing conformational changes to stimulate the PD to function [17]. In VSD, the S4 helix is composed of many positively

charged residues. Especially, there are four to eight arginines which are highly conserved along the S4 helix. These conserved arginines are involved with the voltage sensing mechanism of the VSD. Thus the movement of the S4 segment is an important and intensive research subject for understanding the molecular basis of voltage sensing mechanism. The opening and closing of the channel gate is relied on the functional and conformational couplings between the voltage sensor domain and the pore domain.

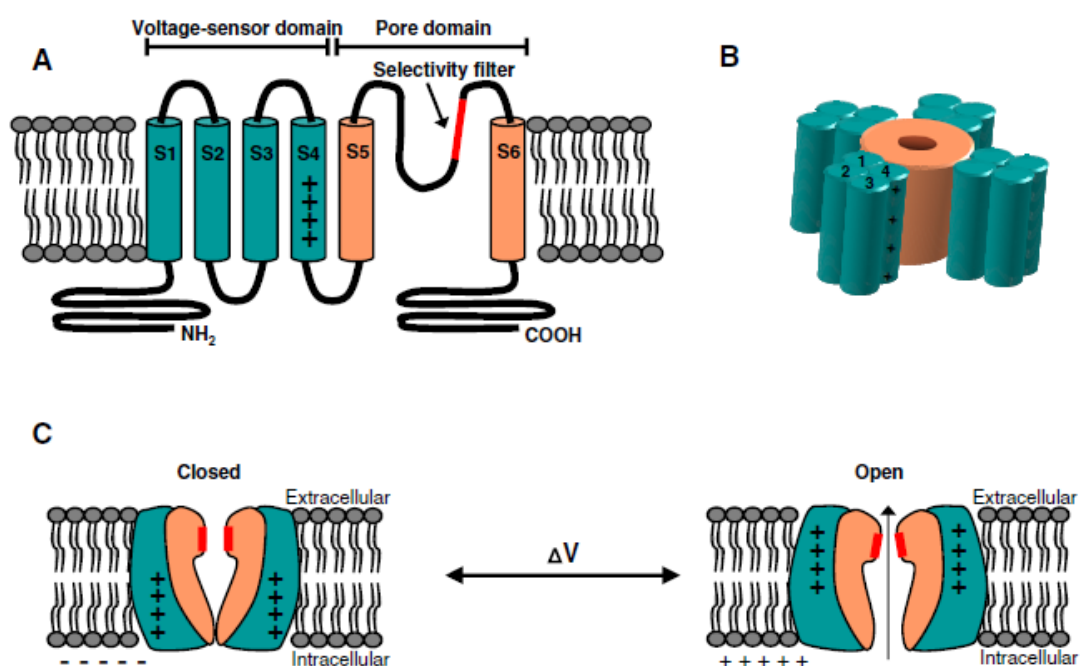


**Figure 1.4** The general structure of voltage – gated ion channels. Each domain is consisted of six transmembrane S1 – S6. The VSD (green) is a positively charged arginines on S4 at every third position. The PD (orange) form S5 - S6 helices that is the region for ions pass through to membrane. And c) when the changing membrane potential to depolarization state, the S4 helix moves outwardly the membrane and results to the PD open [18].

### 1.3 Na<sub>v</sub> channel structure

In eukaryotes, voltage-gated sodium (Na<sub>v</sub>) channel allows sodium ion flux at a rate of  $> 10^7$  ions/s. Therefore, this rate makes Na<sub>v</sub> channels of mammalian being important for the effective transmission of nerve impulses of neurons in the brain, controls the heart rate, contraction of smooth muscles, transmission of various neurotransmitters in the epithelium etc. Because of Na<sub>v</sub> channels are critical to function of neurons, so the Na<sub>v</sub> channels are a molecular target for the treatment of various diseases caused by abnormalities of nervous cells [19].

#### 1.3.1 General molecular structure and transmembrane topology

Most Na<sub>v</sub> channels are homotetramer or heterotetramer. Nevertheless, heterotetrameric Na<sub>v</sub> channels are composed of four homologous domains with a single polypeptide chain. Each domain consists of six transmembrane segments (S1-S6) [20]. The S1-S4 transmembrane segments form a voltage-sensing domain (or VSD) and a pore loop structure is connected with S5 and S6 helices, or called pore domain (PD) [21]. The S4 transmembrane segment contains of positively charged amino acids, arginine or ARG, which is shown as a voltage-sensing. As shown in Figure 1.5.

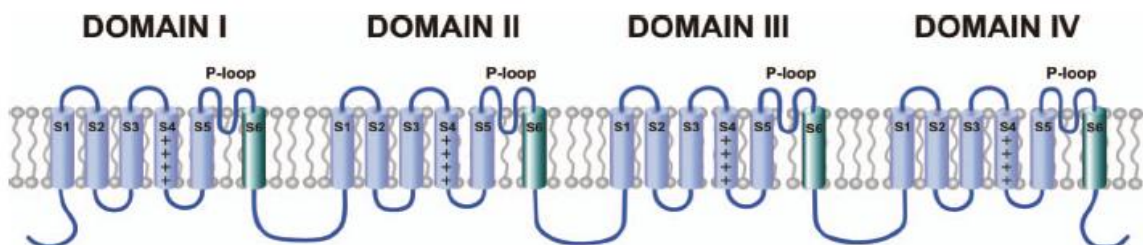
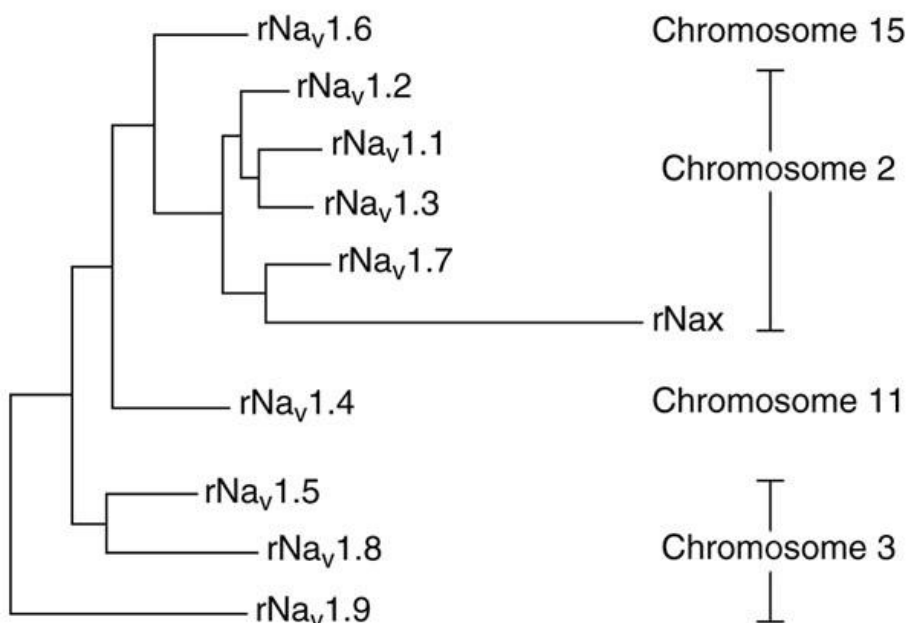


**Figure 1.5** The structure of Na<sub>v</sub> channels are a homotetramer that composed of four domain. Each monomer is consisted of the six transmembrane (S1 – S6) [22].

### 1.3.2 The Na<sub>v</sub> family

Voltage-gated sodium (Na<sub>v</sub>) channels were the member of the superfamily ion channels which consists of voltage-gated potassium channels and voltage-gated calcium channels. Na<sub>v</sub> channels can divided into four groups. The first group is composed of Na<sub>v</sub> 1.1, Na<sub>v</sub> 1.2, Na<sub>v</sub> 1.3 and Na<sub>v</sub> 1.7 which located on chromosome 2 in both human and animal. The second group of the channels Na<sub>v</sub> 1.5, Na<sub>v</sub> 1.8 and Na<sub>v</sub> 1.9 are located in human chromosome 3p21-24 and chromosome 3 in animal. The last two group are Na<sub>v</sub> 1.4 and Na<sub>v</sub> 1.6 which located on human chromosome 11 or animal chromosome 17 and human chromosome 15 or animal chromosome 12 [23], respectively, as shown in Figure 1.6



**Figure**

**1.6**

The voltage – gated sodium channels can be classified into four groups by location on human chromosome [23].

### 1.3.3 Role in action potential

The voltage potential of the nervous cells is determined by the difference between the concentration of ions inside and outside of cell membranes. At the resting state, membrane voltage is approximately  $-70$  mV. When the nervous cells are stimulated, the voltage potential is changed due to the sodium channels open and sodium ions rapidly flow inside cell membranes, so the voltage potential of nervous cells became more positive values. This stage is called depolarization stage [24-25]. When sodium ions flow into the membranes until the voltage potential reaches its peak, sodium channel gates are closed and potassium channel gates open, allowing potassium ions flow out of the cells. This changing state is called repolarization stage [26]. And when the voltage potential is reduced to less than the resting state, this changing state is called hyperpolarization, as shown in Figure 1.7. At this state, all  $\text{Na}_v$  and  $\text{K}_v$  channels are inactive and no ion flows through these channels. After hyperpolarization, the Na-K pump returns the voltage potential back to the resting potential again [27].

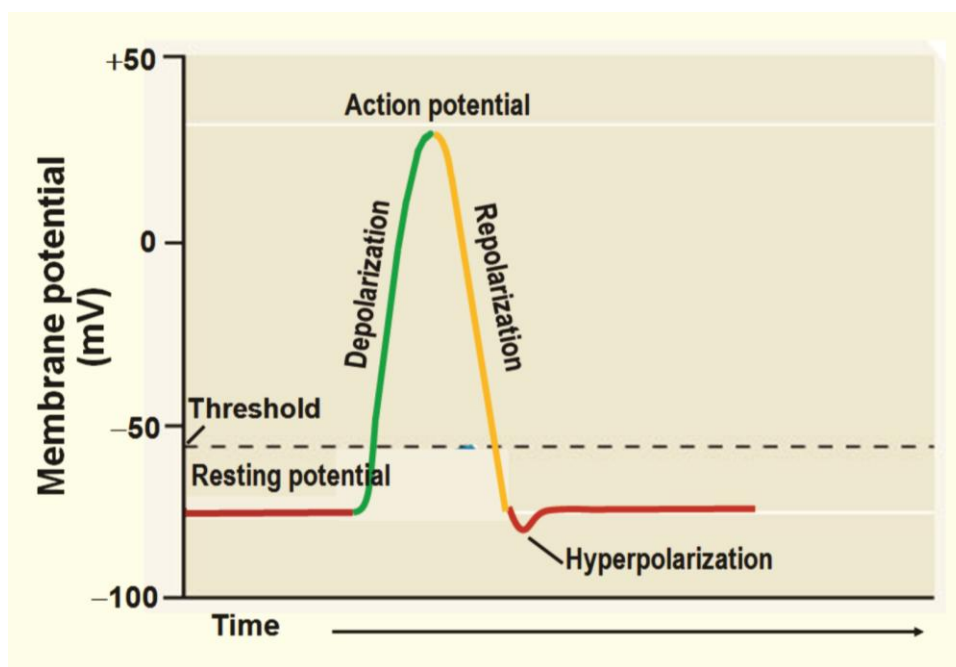


**Figure 1.7** The action potential of nervous cells.

## 1.4 Literature reviews

### 1.4.1 Discovery of the first Na<sub>v</sub> channels

The first bacterial sodium channel was identified from the bacterium *Bacillus Halodurans* (NaChBac). Ren and coworker [28] discovered that this channel function as a voltage-gated ion channels. The main structure of NaChBac is the same as a mammalian putative voltage-gated cation channel of sperm (or CatSper). The amino acid sequence of NaChBac is similar to a voltage-gated calcium channels, especially the pore region. Although the sequence alignments are similar between Na<sub>v</sub> and Ca<sub>v</sub> channels, NaChBac is also highly specific for the selection of the sodium ions. Na<sub>v</sub> channels of eukaryotes are complex proteins composed of a single polypeptide chain that form four homologous domains. The eukaryotic voltage-gated calcium and sodium channels have 24 transmembrane helices with four homologous domains, whereas NaChBac is homotetramer with six transmembrane helices per monomer. NaChBac is the simple Na<sub>v</sub> channel, and therefore presents a good model for structural study to understand the fundamental mechanism of voltage-dependent channel in mammalian.

### 1.4.2 Molecular basis and transmembrane topology of NaChBac

NaChBac has been one of the most well characterized Na<sub>v</sub> channel owing to their availability for expression and functional characterization. To date there is no crystal structure of NaChBac. NaChBac is a homotetramer, each monomer is consisted of six transmembrane segments (S1-S6) which have been divided into two parts. The first part contains four transmembrane segments, S1, S2, S3 and S4, called voltage-sensing domain (VSD), and the second part consists of two transmembrane segment, S5 and S6. The tetrameric association of these two segments forms the central pore domain (PD) [29-31], as shown in Figure 1.8.

The S4 helix plays a key role as a voltage sensor. In NaChBac, it consists of four positively charged arginines at every third position [32]. For the stability of the S4 in low



dielectric membrane, these arginines must form either hydrogen bond with water or lipid head groups or salt-bridge with negatively charged residues or both. It must move outwardly or inwardly to respond membrane voltage changes to adjust the positively charged residues in the hydrophobic environment under the electrical potential of membrane [33]. The S4 motion results in changing interactions of arginine salt-bridges.

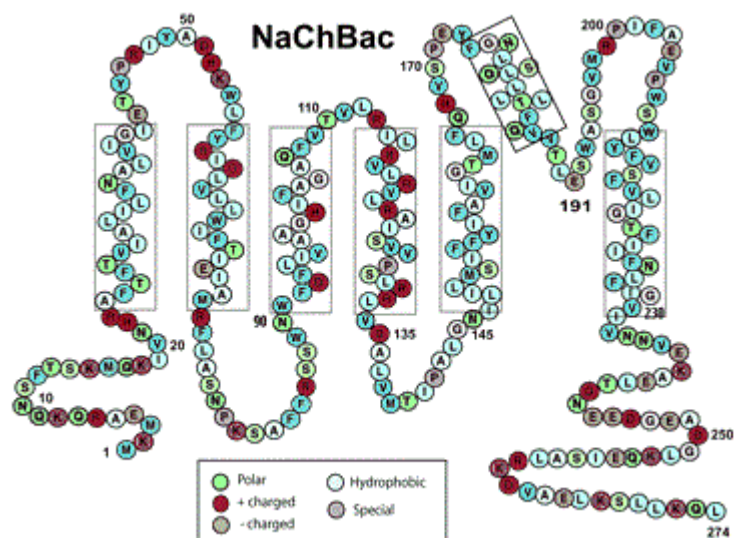


**Figure 1.8** Transmembrane topology of NaChBac [34].

### 1.4.3 Voltage sensor domain: the functional independent domain

In 2003, Jiang and coworker [35] have reported two crystal structures of voltage-dependent potassium channel from *Aeropyrum pernix* or KvAP channel. One is the structure of full-length KvAP channel and the other one is the separate voltage sensor domain. They showed that the isolated VSD is structurally stable in detergent and still functional as voltage sensor. From the structure of KvAP channel, they found that the pore domain exhibits very few contacts with its own chain but it interacts with the VSD of the other monomer instead. They concluded that the VSD is the functional independent domain. Later, several reports showed evidences that support this conclusion. For

instance, Chakrapani et al. confirmed that the isolated – VSD can be reconstituted in membrane environment and remain monomeric without disrupting and perturbing the three dimensional architecture [38]. In addition, the discovery of two proteins showed that the VSD involved with enzymatic activity and ion permeation. This includes voltage-sensitive phosphatase or Ci-VSP from *Ciona intestinalis* [36] and voltage-sensitive proton (H<sup>v</sup>) channels [37]. This finding revealed that VSD is not exclusively belonged to ion channels. This implies that the isolated-VSD has its own function. The study of the isolated VSD will provide a basic model system for structural and dynamical studies to understand the general principles of voltage sensing.

### **1.5 Voltage sensing mechanism: how does the voltage sensor move?**

Generally, neurons in the resting state have a voltage potential about -70 mV. which sodium channels are closed and when the urge to make a positive potential which causes sodium channels to open and a high sodium ions concentrations on the extracellular are rapidly flow into the cells, making the value voltage of -70 to 30 mV., this stage is called depolarization stage.

At the depolarization stage, the opening of the pore domain of sodium channels are associated with changes in the conformation of VSD, especially the S4 segment. Because of the S4 segment is composed of arginine (or lysine) four to eight residues which is positively charged. When the S4 segment moves to outer cell membrane, resulting in the PD open at depolarization stage, and when the S4 segment moves into the interior of the cell membrane, the PD are also closed at the resting stage [38-40].

The motion mechanisms of the S4 segment in VSD is still controversial. There are the three main models [41] such as (i) the paddle model, (ii) the transporter model, and (iii) the helical screw model as shown in Figure 1.9. The helical-screw model, the S4 helix is located in the crevices within the intracellular membrane in resting stage. When the changing the membrane potential to depolarization stage, the S4 helix is rotated and translates along its axis toward the extracellular membrane with distance about 13 Å and

rotated about  $60^\circ$ . The transporter model, the S4 helix is located in the crevices contact with the intracellular membrane at resting state. When the changing voltage membrane in depolarization state, the S4 helix can be tilted and rotated about 2-3 Å contact with the extracellular membrane but does not across the membrane as a result reshape allow charges across membrane. This motion model is a rotate in place and moving orifice. The paddle model, the S4 helix forms a paddle that is moving through membranes. At resting state, the S4 helix that is embedded in the intracellular membrane when the membrane potential in depolarization state, the S4 helix will be repositioned to the outer membrane and moves about 15-20 Å.

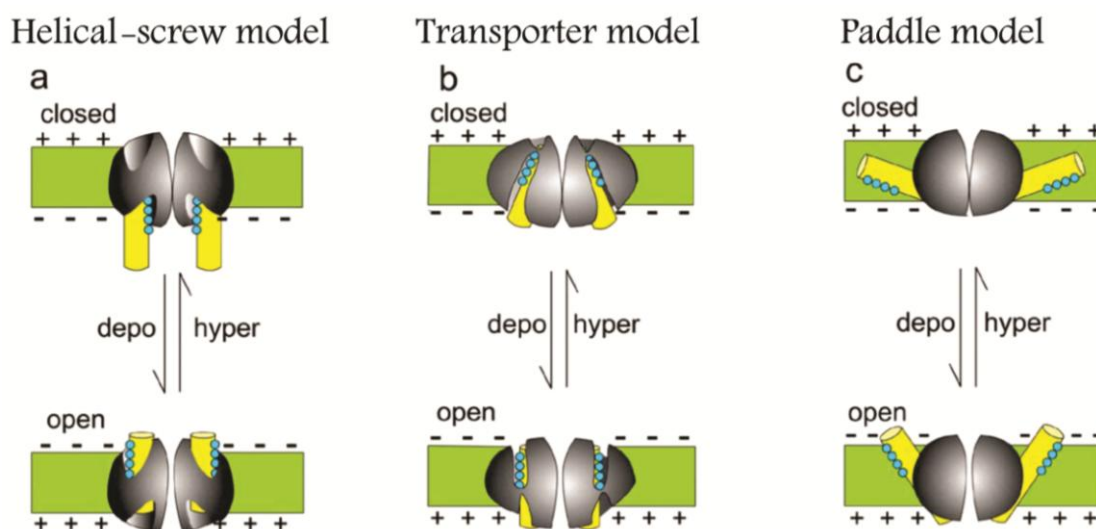


**Figure 1.9** The motion mechanisms of the S4 segment in VSD. From left to right, a) the helical – screw model, b) the transporter model and c) the paddle model [42].

In 2010, Chakapani and coworker [43] studied the isolated-VSD of NaChBac in activated (Up) state by using PaDSAR and EPR techniques. They found that the NaChBac – VSD is stable in membrane environment and closely behavior with the KvAP, Kv1.2 and Kv1.2 – 2.1 channels. Paldi et al. [44] proposed that the motion of the S4 helix is likely to be the helical-screw model with a rotation of  $\sim 60^\circ$  and a translation

~4.5 Å. As a result, the S4 arginines made changes in salt-bridge interactions in NaChBac mutant affecting VSD conformation in the resting (Down) states. Based on the crystal structure of voltage-gated potassium channels, they predicted that in the Down state residue on S1 helps to stabilize positively charged on S4 by the electrostatic coupling between negatively charged residue (E43) on S1 and positively charged residues (R113 and/or R116) on S4. They predicted that the interaction between E43 with R116 help to stabilize the Up conformation whereas the Down conformation is associated with a salt-bridge interaction between E43 and R113. Nevertheless, the Down state conformation of VSD is still not known.

## **1.6 The objectives of this research**

The main objectives of this research are as follow :

1. To build structural model of the voltage-sensing domain of NaChBac channel in putative activated (Up) and resting (Down) states based on available experimental data reported in the literatures..
2. To investigate structure and dynamic properties of the voltage-sensing domain of NaChBac channel in the putative Up and Down states by using molecular dynamics simulation.

## CHAPTER II

### MATERIALS AND METHODS

#### 2.1 Materials

##### 2.1.1 Hardware

Personal computers and the high-performance computing cluster “Pheonix” located at Floor 11th, Mahamakut Building, Department of Chemistry, Faculty of Science, Chulalongkorn University were mainly used to carry out this work.

##### 2.1.2 Software

###### *The NAMD 2.7b program*

The NAMD2.7b is a program for design biomolecular systems to molecular dynamic (MD) simulations. For using NAMD2.7b program needs (i) Protein data bank (or PDB) serves atomic coordination and velocities of systems which loaded the protein data from <http://www.pdb.org>, (ii) Protein structure file (or PSF) serves a structural information of the protein such as atoms, bonds, and angles, (iii) Force field parameter files are used to describe the potential energy of molecular systems. They are CHARMM and AMBER, and (iv) Configuration files are used to set all the options to run a simulation with NAMD [45].

###### *The Visual molecular dynamics (VMD)*

VMD is a visualization program for biological systems and can be used to analyze the results of MD simulations, especially MD trajectories produced by the program NAMD.

### ***The program SSH secure***

SSH secure is a program for login, transferring a file and execute commands to connect to any server. It is used instead of rlogin, TELNET and rsh because of security reasons.

### ***The program APBS***

APBS is a software for calculating the molecular solvation energy in biological systems based on solution of the Poisson – Boltzmann equation (PBE). This software is performed to describe interactions between the structural model in membrane and aqueous media with help of a java scripts. And the PQR file is required for this program [46].

### ***The PDB2PQR program***

The PDB2PQR is a python software which use to add hydrogen atom with assign atomic charges and radii. The PDB2PQR is used to prepare the structural model for the APBS calculation.

## **2.2 Methods**

### **2.2.1 Modeling of NaChBac-VSD in the Up state**

Although a structure model of NaChBac–VSD in the activated (Up) state was previously done and not in this thesis framework, relevant information on how the model was constructed is provided for comprehension [43,47], as shown in Figure 2.1. The modeling methodology was based on a knowledge-based model building approach, and subsequently refined using the previously developed method, Pseudoatom-Driven Solvent Accessibility Refinement (PaDSAR). In brief, a homology model of NaChBac-VSD was built based on the activated-state Kv1.2-2.1 chimera crystal structure and

transmembrane prediction data. To construct the system for refining the model, the individual C $\alpha$  atom was attached by one of the four spin-labeled pseudoatom types (lipid-exposure or water-exposure, or water-lipid interface and buried site), of which each type was selected according to the interpretation of a total of 118 EPR-derived residue environmental data. The pseudoatom-attached model was subsequently embedded in membrane system containing pseudoatoms of oxygen in the lipid phase and pseudoatoms of nickel complex in the aqueous phase. In the PaDSAR structural refinement, several cycles of energy minimizations and molecular dynamics simulations with EPR-derived restraints were performed to generate an ensemble of structures. In addition to the calculation of restraint potential of pseudoatoms, the CHARMM19 polar hydrogen force field was also employed for calculating interaction between protein atoms. The model was chosen from an ensemble of structures in a way to meet the best fit for given accessibility data obtained from SDSL/EPR.

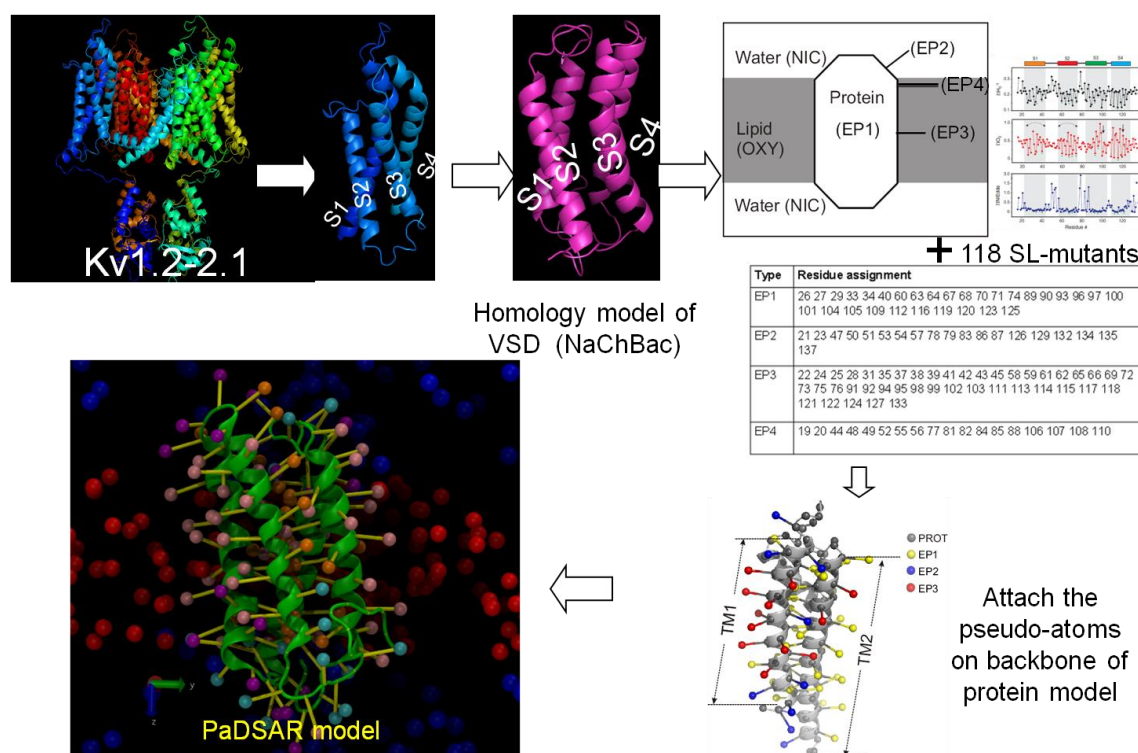


**Figure 2.1** Methodology flow chart for constructing structure model of NaChBac-VSD [43,47].

### 2.2.2 Modeling of NaChBac-VSD in the intermediate and down states

The resulting model in activated state was taken as initial structures for modeling at the intermediate and down states. In this study, we prepared four models which is one model in the intermediate and the other three models in down states. The four models of the VSD-NaChBac have been created based on the helical-screw model. This was done by rotating and sliding the S4 helix along its axis into the intracellular cells. For constructing structure model of the intermediate state, or int, the S4 helix was rotated in the direction that the guanidium group of the arginine116 (R2) side chain form salt-bridge or hydrogen bond interaction with the carboxylate group of aspartic60 (D60) of S2. Structure models of the down state were made the same as the intermediate state, but the carboxylate group of D60 of S2 form salt-bridge interaction with the guanidium group of the arginine113 (R1) side chain. The recent research reported that the salt-bridge interaction between was formed glutamic43 (E43) of S1 with R1 of S4 in the down state. Therefore, we used the data to build models at the down state. The first structure model in the down state, Dwn<sub>1</sub> or Down<sub>1</sub>, R1 side chain of S4 form salt-bridge interaction with D60 of S2 by rotating S4 helix. The second structure model in the down state, Dwn<sub>2</sub> or Down<sub>2</sub>, the side chain R1 of S4 form salt-bridge interaction with E43 of S1 and D60 of S2. The third structure model in down state, Dwn<sub>3</sub> or Down<sub>3</sub>, the salt-bridge interaction was similar to the Dwn<sub>2</sub> model, but the difference between them is the amount of movement of S1 helix. All the structure models were prepared for energy minimization and molecular dynamic (MD) simulation to the distortion of the structures and bonds.

### 2.2.3 Calculating electrostatic solvation free energy

Electrostatic solvation free energy is required to transfer the voltage sensing domain from aqueous media into the membrane bilayer [48]. Amount of the electrostatic solvation free energy for the transferring of voltage sensing domain from aqueous media into the membrane bilayer was obtained by subtracting the electrostatic solvent energy



of the VSD in membrane with a low dielectric on environment ( $\Delta G_{\text{elec,membrane}}$ ) from that in bulk water with a high dielectric environments ,

$$\Delta G_{\text{elec}} = \Delta G_{\text{elec,membrane}} - \Delta G_{\text{elec,water}}$$

The program adaptive Poisson – Boltzmaan solver (APBS) 1.2.1 [49] with help of a java-based graphical user interface APBSmem for setting up input parameters were performed for the electrostatic solvation free energy calculation of all five of NaChBac – VSD models. Program VMD and command scripts were used for the transformation of atomic coordinates. Adding the hydrogen atom together with assigned atomic charges and radii were using the PDB2PQR program. The CHARMM22 parameter sets was used for partial atomic charges and radii of three resolution maps for a solving PBE : 300 x 300 x 300 Å for coarse, 200 x 200 x 200 Å<sup>3</sup> for medium and 100 x 100 x 100 Å<sup>3</sup> for fine and all

maps were used a grid point within 161 x 161 x 161. The implicit membrane slab was introduce to model in the Cartesian xy – plane and bilayer is aligned along the z – axis. The range of membrane bilayer ( $L_{\text{mem}}$ ) thickness was around 30 – 40 Å. The dielectric constants for the membrane ( $\epsilon_{\text{m}}$ ) and water ( $\epsilon_{\text{w}}$ ) was 2 and 80, respectively.

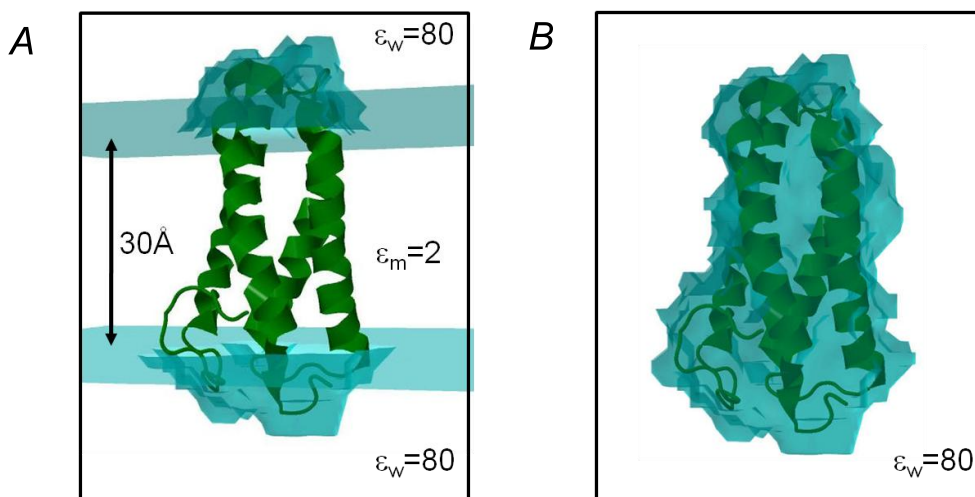


**Figure 2.2** Model systems used to compute electrostatic free energy of protein solvation. (A) The VSD is embedded in the membrane. The membrane region between the two blue planes is assigned a dielectric value  $\epsilon_m = 2$ . Bulk water above and below the membrane is assigned a dielectric value of  $\epsilon_w = 80$ . (B) The VSD in the bulk water ( $\epsilon_w = 80$ ) without the membrane. The protein solvation energy is calculated by  $\Delta G_{\text{elec}} = \Delta G_A - \Delta G_B$ .

### 2.2.4 Molecular dynamics simulation

Molecular dynamic (MD) simulation is a computational method which describes structure of dynamics and thermodynamics properties are used to study proteins and biological systems, generates data at the microscopic scale [50]. The characterization of the molecular motion and energy are directly received from the interaction between molecules. Behavior of the molecular motion is based on the function of time and generates configurations by using the Newton's equation, ( $\Sigma F = ma$ ), and from position of molecules can also lead to the thermodynamic properties. The data used for MD simulation techniques have included the chemical, ensemble, potential force field and simulation time, resulting in a relative position of the molecules which can be used to determine the thermodynamics properties.

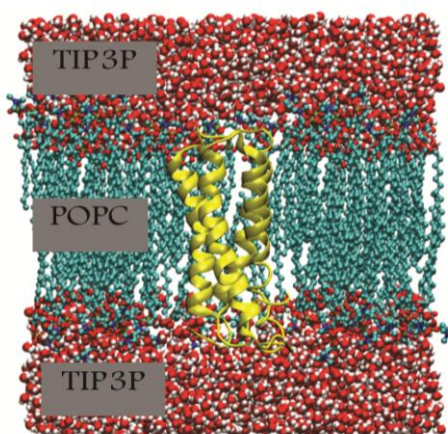


**Figure 2.3** The membrane proteins system, Palmitoyl oleoyl phosphatidyl Cholines are membrane bilayer and TIP3P are force field parameter for water molecules.

All five models were used to provide a system that consist of a membrane and water using the Visual Molecular Dynamic (VMD) program : one model in the activated state, one model in the intermediate state and the other three model in down state. All five structure models were embedded in a palmitoyl oleoyl phosphatidyl cholines (POPC) membrane bilayer and TIP3P waters, example as shown in Figure 2.3. The protein systems were neutralized by the addition of sodium ions for the negatively systems and chloride ions for the positively systems using the VMD program.

MD simulations of all five models were carried out using the NAMD2.7b program. CHARMM 22 and CHARMM 27 were used as a force field parameter for proteins and lipids, respectively. TIP3P parameter was used for waters. Molecular modeling has a periodic cell size  $78 \times 78 \times 81 \text{ \AA}^3$ . The system was run at constant temperature of 300 K and constant pressure of 1 atm. Langevin dynamics (LD) was used for controlling the temperature of the system and the system was controlled the pressure by using a Noé-Hoove Langevin Piston.

To avoid any instability of the starting configuration, the system was subjected to 3 successive cycles of energy minimizations and restrained MD simulations. During the first restrained MD run, only lipid tails were allowed to move. For the subsequent run, harmonic restraints were imposed only on the protein, and left the rest of the system unrestrained. The third cycle was performed by applying harmonic restraints on the protein and forces to water molecules for not entering the membrane region. Each MD simulation was performed for 0.5 ns with an integration time step of 2 fs. The preparation protocol as described above was processed in order to relax the conformation, remove bad contacts due to steric overlap, and permit a proper assembly of lipids, water, ions and the protein. Each system was computed in the MD simulations at 50 ns. The integration time steps of 2 fs. was used. The configurations and velocities were stored every 2 ps.

### **2.2.5 Analysis of MD trajectory**

Analysis of the trajectories MD simulation using VMD program includes the root-mean square deviation, (RMSD), the root mean square fluctuation (RMSF), hydrogen bond profile of S4 arginines, secondary structure profile and solvent density profile.

## CHAPTER III

### RESULTS AND DISCUSSION

#### 3.1 Primary structure and sequence alignment of NaChBac-VSD

The alignment between NaChBac-VSD and Kv-VSD sequences is shown in Figure 3.1. This sequence alignment is used to develop the model of the activated state. With an exception of the S4 segment, the alignment of transmembrane regions including S1, S2 and S3 captures mostly hydrophobic residues. Only few charged residues remain inside the transmembrane segments. For instance, D60 and E70 in S2 are found to be conserved between NaChBac-VSD and Kv-VSD sequences. This suggests that transmembrane voltage sensor residues are conserved within voltage-gated ion channel superfamily.

More attention has been focused on the alignment of S4 segment because it contains highly conserved arginines with a repeating pattern of tripeptide, (RXX)<sub>n</sub>. For NaChBac-VSD, there are four arginines, R113, R116, R119 and R122, hereafter referred to as R1, R2, R3 and R4, respectively, located at every third position along the S4 helix. However, the number of the positively charged residues (arginine or lysine) of the S4 segment is not equivalent between Na<sub>v</sub> and K<sub>v</sub> channels. The S4 of K<sub>v</sub> appears to contain a repeating pattern of the conserved arginines longer than that of NaChBac. In Kv1.2-2.1 crystal structure, the repeating arginine pattern starts from Q1(=Q290), R2(=R293), R3(=R296), R4(=R299) and R5(=R302) [51]. Since a homology model is built based on a structure template derived from the x-ray structure of Kv1.2-2.1 chimera, the template (Kv1.2-2.1) sequence is considered to be high priority for aligning with the NaChBac sequence. Therefore, those four arginines of NaChBac, R113, R116, R119 and R122, are aligned with R293, R296, R299 and R302 of Kv1.2-2.1 chimera, respectively.

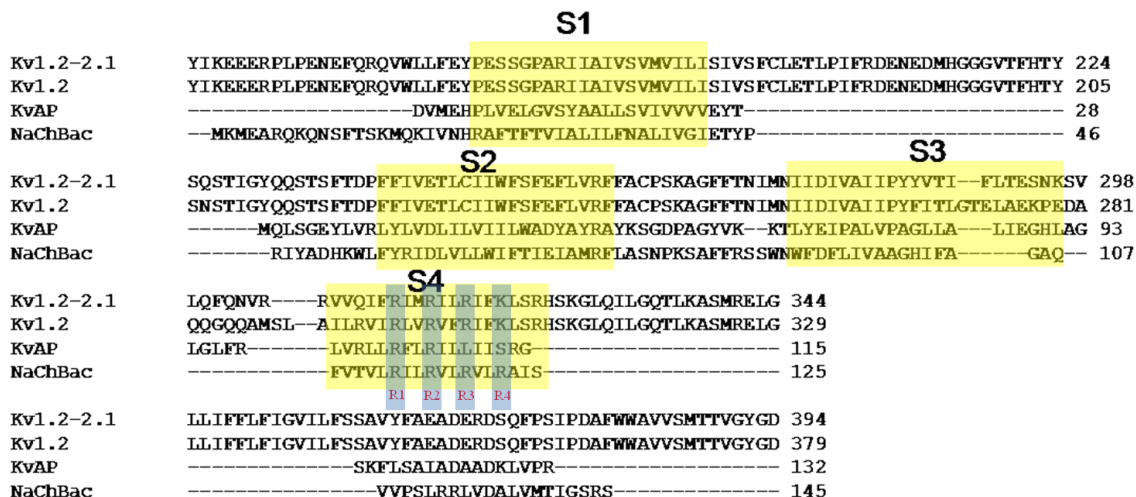


**Figure 3.1** The sequence alignments of VSD – NaChBac are compared with Kv1.2 – 2.1, Kv1.2 and KvAP and the S4 helix consists of arginine or lysine at every third positions. The S1 – S3 helices have been a negatively charged residues that form salt – bridge interactions with the positively charged residue on S4.

### 3.2 Structure model in the activated state

The activated or “up” state conformation of NaChBac-VSD consists of residues starting from Q17 to S145. For an overall tertiary fold of the model, the four TM helices are packed antiparallel in counterclockwise order as shown in Figure 3.2. Only the guanidinium of the first arginine, R113, lines completely outside whereas that of R116 has partial contact to the environment. The side chain of the last two arginines, R119 and R122 are in the membrane and face to the core of the VSD bundle. The intracellular half of the S4 helix of the up state model has a  $3_{10}$  helix character. The electrostatic potential on the solvent accessible surface of VSD reveals global features of distribution of hydrophobic, negative and positive charge on the molecule. The longest loop is about 15 residues long connecting between S1 and S2 in the extracellular side. The S3-S4 loop forms a short helical hairpin structure.

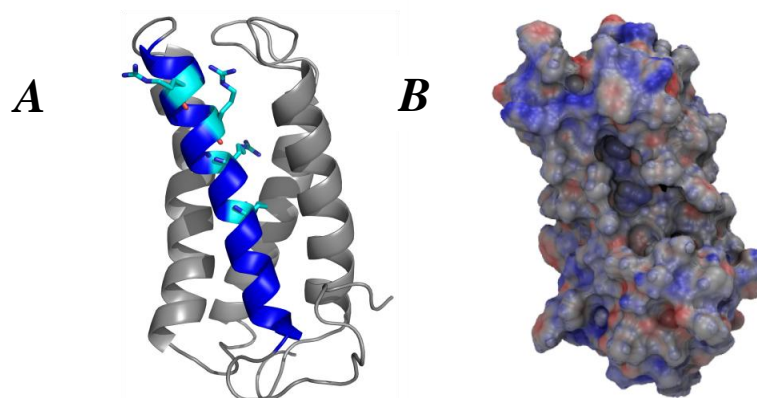


**Figure 3.2** Structural model in the up state is shown in (A) cartoon model (B) surface model with electrostatic potential

Structural model of NaChBac – VSD is similar to the activated state structure of known 3D structures of  $K_v$  channel voltage sensors, as shown in Figure 3.3. This suggested that the VSD is conserved across voltage-gated ion channel superfamily. The conserved-VSD also implies the intrinsic function as a voltage sensor.

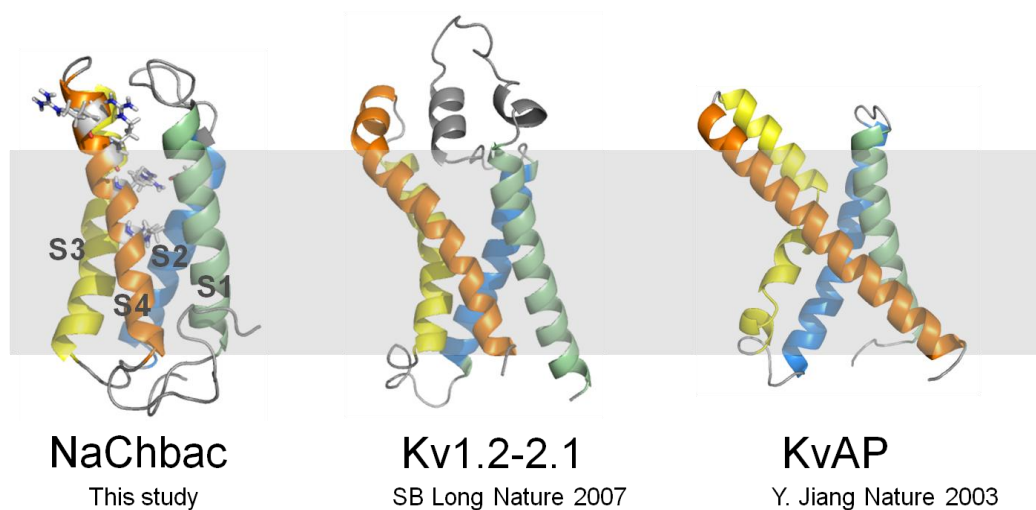


**Figure 3.3** Comparison of VSD structures:  $Na_v$  versus  $K_v$

During the work being carried out, the first crystal structure of voltage-gated sodium channel from the bacterium *Arcobacter butzleri* (NavAb) has been published in Nature 2011 [52]. The NavAb channel voltage sensor is in a “pre-open” state, with its voltage sensors activated, but the pore closed. By comparing the VSD structures, an arrangement of the four transmembrane segments of NaChBac remains quite similar to that of the NavAb as indicated by the backbone RMSD of 2.1 Å, as shown in Figure 3.4. Comparison of transmembrane helices of the VSD between our model and NavAb crystal structure revealed a similar length for S1, one helical-turn shorter for S2 and a longer length for S3 and S4. A substantial difference is that only intracellular half of the S4 helix of our model exhibits a  $3_{10}$  helix character, as shown in Figure 3.4, whereas the entire S4 segment of NavAb adopts  $3_{10}$ -helical conformation. Based on the experimental and theoretical studies, the presence of  $3_{10}$  helix contents would facilitate the S4 motion toward a down state

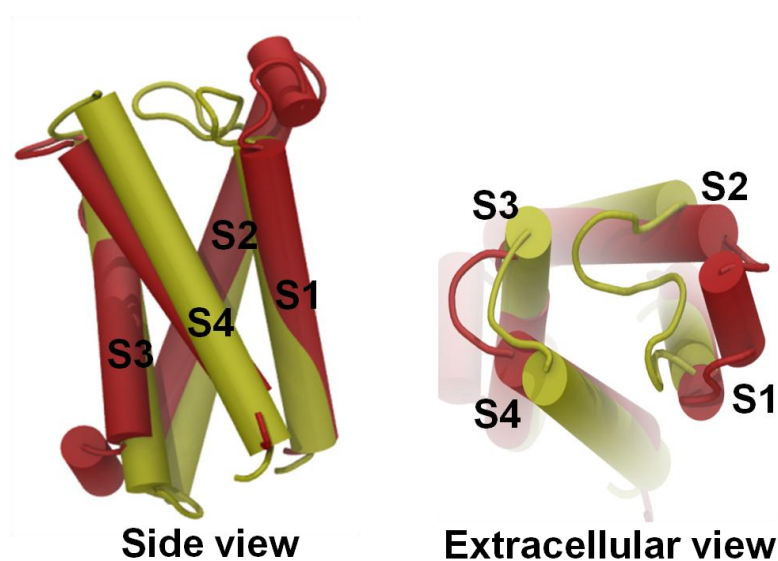


**Figure 3.4** Comparison of VSD structures: NaChBac (yellow) *versus* NavAb (red)



### 3.3 Structure models in the down and intermediate states

The assessment of model candidates such as the salt-bridges of S4 arginines together with the minimum free energy of membrane solvation has provided three plausible structures (denoted as *Down*<sub>1</sub>, *Down*<sub>2</sub> and *Down*<sub>3</sub>) for a NaChBac-VSD down state conformation, as shown in Figure 3.5. These model buildings showed that side chains of the two outermost S4-arginines (R113 and R116) face toward the VSD core which is consistent with cell complementary assays and the sulfhydryl accessibility studies. These models captured an important feature that is a substitution of key salt-bridge interactions associated with S4 arginines. Here distance proximity and an angle criteria of H-donor and H-acceptor were used to indicate a potential salt-bridge formation. In the up-state model, R119 and R122 formed respectively a salt-bridge with D60 and E70 while R113 and R116 would most likely be surrounded by a hydrophilic environment. A salt-bridge of R119-D60 was apparently displaced by a counter-charge neutralization formed between either R113 or R116 and D60 to compensate for the arginines dipping into the lipid bilayer. Especially for *Down*<sub>2</sub> and *Down*<sub>3</sub> models, a cluster of salt-bridges interactions involving the two outermost arginines and D60 and E43 was observed. A similar salt-bridge reformation was also observed in a simulation study of the resting-state model of KvAP-VSD. In *Down*<sub>1</sub> and *Down*<sub>3</sub> models, it appears that R119 can reform a salt-bridge with D93 of S3 located about one and a half helical turn lower, with respect to the D60 position, and R122 can form a salt-bridge with E70 of S2. Such interactions were not found in *Down*<sub>2</sub>. A noticeable difference between *Down*<sub>1</sub> and *Down*<sub>3</sub> lies in the different orientation of the S1 helical phase. Apparently, E43 of S1 of *Down*<sub>1</sub> likely faces outside the VSD core while that of *Down*<sub>3</sub> lies toward the central line of an inner crevice of VSD. Besides similar changes of the salt-bridge for the arginine residues, the selected models revealed further structural similarity in terms of a minimum lipid exposure of the four arginines, a small movement of S2 and S3 and an opening cavity of the VSD core, particularly at the intracellular half of the membrane. Particularly, the *down*<sub>3</sub> model showed that all four arginines participate in salt-bridges with acidic residues of S1, S2 and S3.

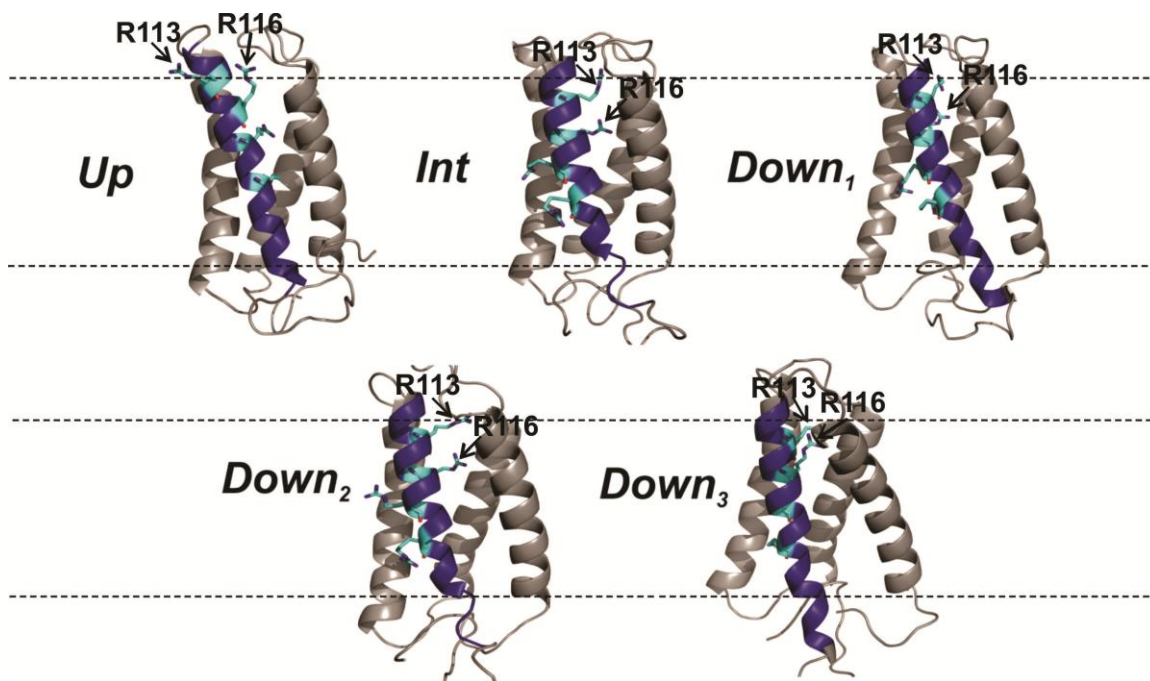


**Figure 3.5** Structure models of the up, intermediate and down states of NaChBac-VSD

Furthermore, we observed a model, of which the salt bridge of R119-D60 was no longer but it was substituted by the next gating charge arginine R116, as shown in Figure 3.5. This salt-bridge interaction between R116 and D60 may correspond to a conformational stage at which the voltage sensor S4 transits between the up and down state. Therefore, we consider this model as a conformational intermediate (*Int*) between the up and down states of NaChBac-VSD. Structural superposition between the intermediate and up conformations results in RMSD of 2.4 Å. In this intermediate, the displacement of the S4 charges normal to the membrane plane is  $\sim 3\text{Å}$  with respect to the up model, suggesting a small movement of the gating charge.

### 3.4 Electrostatic solvation free-energy by Poisson – Boltzmann solvent continuum method

#### 3.4.1 Electrostatic solvation energy of NaChBac-VSD as a function of $\epsilon$ and membrane thickness

Electrostatic free energies of protein solvation were calculated for the voltage sensor domain of NaChBac, KvAP, Kv1.2-2.1 and NavAb. The results show that all protein solvation energies are positive. This indicates that for a spontaneous change the protein needs the energy to do work. In other words, the insertion of VSD from bulk water to the membrane needs an external driving force. As shown in Table 3.1, an increase of membrane thickness results in an increase of the protein solvation energies. However, the solvation energies decrease upon an increase of protein dielectric.

**Table 3.1** Electrostatic solvation energies of NaChBac-VSD as a function of  $\epsilon$  and membrane thickness ( $L_{\text{mem}}$ )

$\epsilon_{\text{protein}}$	$L_{\text{mem}}$ (Å)	$\Delta G_{\text{elec}}$ (kcal/mol)
2	30	136.2
2	35	195.0
2	40	296.4
4	30	91.5
4	35	134.3
4	40	201.7
10	30	48.5
10	35	72.2
10	40	114.0

### 3.4.2 Solvation energies of $K_v$ and $Na_v$ voltage sensors

The solvation energies of the  $K_v$  and  $Na_v$  voltage sensors, as shown in Table 3.2, follow the order:  $Kv1.2-2.1 < NaChBac < NavAb < KvAP$ . The solvation energy was decomposed into partial contribution of each residue. Apparently, the energies were mainly contributed from the solvation of transmembrane residues rather than that of non-transmembrane residues, as shown in Figure 3.6. Particularly, the S4 segment of  $K_v$  and  $Na_v$  contributes significantly to the solvation energy.

**Table 3.2** Electrostatic solvation energies of  $K_v$  and  $Na_v$  voltage sensors ( $\epsilon_{\text{protein}} = 4$ ,  $L_{\text{mem}} = 30 \text{ \AA}$ )

Type	$\Delta G_{\text{elec}}$ (kcal/mol)
KvAP	231.6
Kv1.2-2.1	85.1
NavAb	150.1
NaChBac	91.5
S4 (KvAP)	472.2-458.9 [53]

The solvation free energies of four highly conserved arginines on the S4 segment were shown in Table 3.3. Based on sequence alignment of voltage-gated ion channel homolog, R1, R2, R3 and R4 are the conserved position of arginines on the S4 helix. Arginines that contribute substantially to the solvation free energy include R1, R2 and R4 of KvAP, R2 and R3 of NavAb, and R4 of NaChBac. It appears that these arginines are either highly exposed to the solvent environment or not form salt-bridge interactions with the negative charge residues.

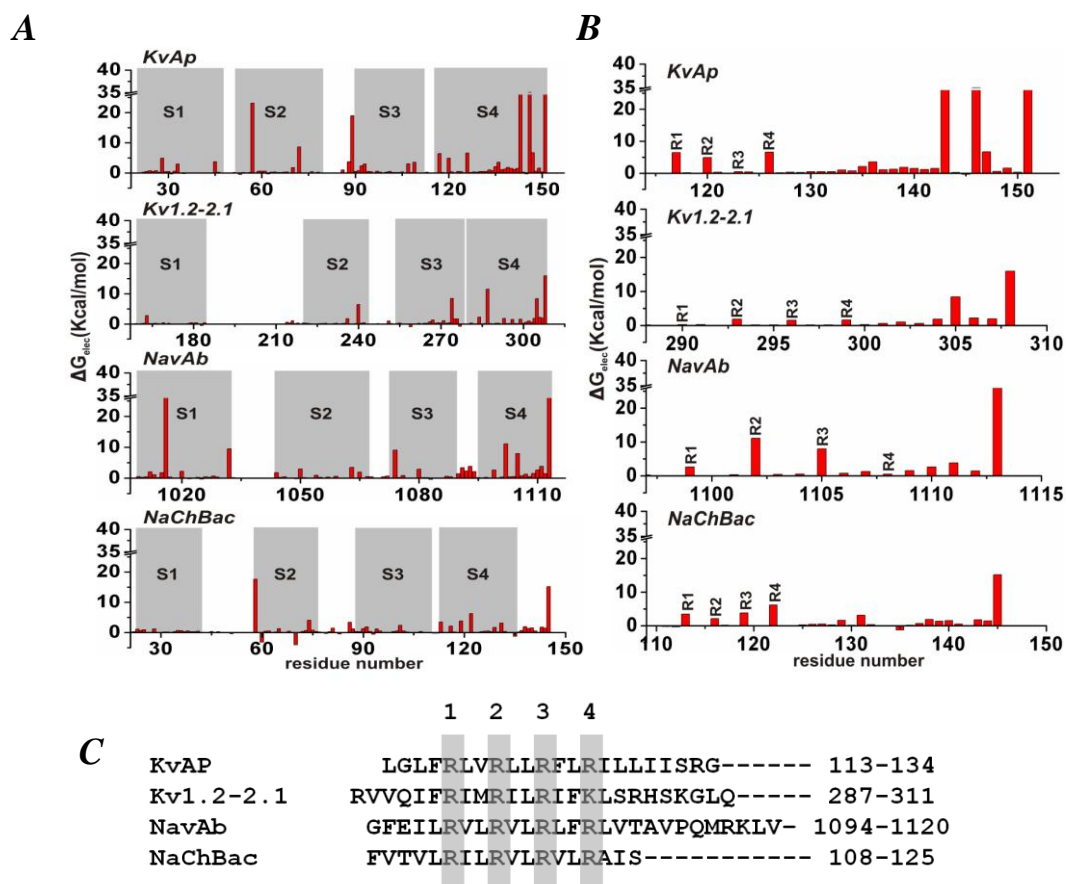


**Figure 3.6.** Per-residue contribution to the solvation energy. (A) all residues of voltage sensor domain, (B) residues on the S4 segment and (C) sequence alignment of the S4 segment.

**Table 3.3** Electrostatic solvation energy of the S4 arginines

Type	$\Delta G_{\text{elec}}$ (kcal/mol)			
	R1	R2	R3	R4
KvAP	6.5	5	0.5	6.5
Kv1.2-2.1	0.4	2	1.2	1.2
NavAb	2.5	11	8	0.9
NaChBac	3.2	2	3.3	6

### 3.4.3 Electrostatic solvation energy of activated, intermediate and open models

A comparison of the membrane insertion energy of the selected models using the solvent continuum method was shown in Figure 3.7. The relative electrostatic free energies of membrane solvation ( $\Delta G_{\text{elec}}$ ) for *int*, *Down<sub>1</sub>*, *Down<sub>2</sub>* and *Down<sub>3</sub>* models were greater than that of the up model. The positive sign of  $\Delta G_{\text{elec}}$  suggested a larger energy barrier for inserting the VSD in membrane-like environment at zero membrane voltage as compared to that of the up model. For the *int* model, the membrane insertion energies was of 30.6 kcal/mole higher than the *up* model. The energy barrier is indeed larger for the conformation toward the down state. Based on a  $\Delta G_{\text{elec}}$  comparison, the *down<sub>3</sub>* model provides the least membrane insertion energies.

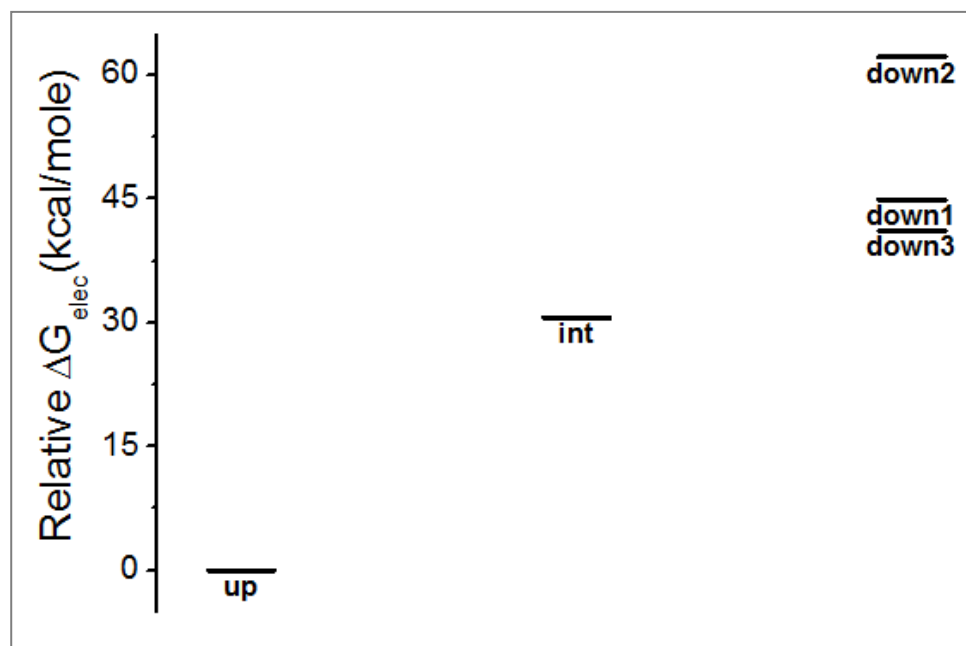


**Figure 3.7** The relative electrostatic free energy of all five states is compared with the up state.

### 3.5 MD simulation of up, intermediate and down models

To further validate the reliability of the models, 50 ns MD simulations of the *Up*, *Int* and *Down<sub>1</sub>*, *Down<sub>2</sub>* and *Down<sub>3</sub>* conformations were performed in explicit solvent environments. MD simulations and the analysis of MD trajectories are described as follows.

#### 3.5.1 Structure and dynamic fluctuation

All of the five MD trajectories were analyzed to determine the stability of the system models. The atomic root-mean-square-deviation (RMSD) function of simulation time was analyzed to determine the equilibrium of the system and stability of the structure, as shown in Figure 3.8, for 50 ns of MD simulations. The black bone RMSD is fluctuated around 3 or 4 Å with respect to the starting model. For the up and intermediate (INT) models, the RMSD values remain stable after 30 ns of simulations. The down2 and down3 models, the RMSD values becomes stable about 10 ns and the down1 model, the RMSD value increase fluctuation and stable after 40 ns of simulation time. From the RMSD of protein backbone of all five states shows that the systems equilibration and structure stability, so we selected the last 10 ns. configurations for property analysis.

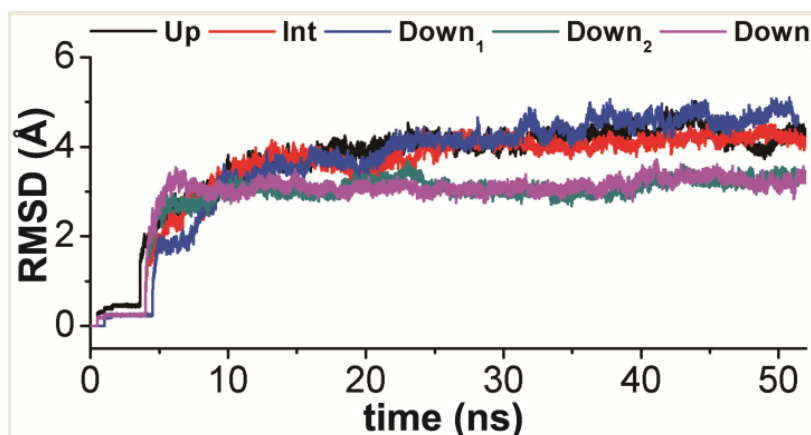


**Figure 3.8** Backbone RMSD with respect to the starting structure of all five MD systems as a function of simulation time.

RMSD of the individual S1-S4 helices of NaChBac-VSD was analyzed to evaluate structure and dynamics of the individual transmembrane segment. RMSDs of the four helices of the up model increase and maintain between 1-3Å relative to the starting structure as shown in Figure 3.9. However, transmembrane voltage sensor in the intermediate and down models shows different structure and dynamics behaviors within the four transmembrane segments during the course of MD simulation. Especially for the intermediate and down state models, distinct structure deviation is observed from larger RMSD values of S3 and S4 helices with respect to those of S1 and S2 helices shown in Table 3.4. Particularly, a major structure deviation of S4 can be observed with a significant increase of RMSD. An interpretation of this result is that the S3 and S4 segments of these models might not be in a stable configuration compared to the S1 and S2 segments. An unstable configuration could be an acceptable explanation for an intermediate state but not for the down state. Therefore, it is essential to find further supporting evidence of structure instability by means of root-mean square fluctuation (RMSF) and secondary structure deformation.

**Table 3.4** RMSD of the individual VSD segments averaged from the last 10-ns MD trajectories.

States	Mean RMSD±SD (Å)			
	S1	S2	S3	S4
<i>Up</i>	1.66±0.13	1.61±0.18	1.91±0.14	2.43±0.11
<i>Int</i>	1.04±0.13	1.38±0.12	2.56±0.08	2.90±0.11
<i>Down<sub>1</sub></i>	1.27±0.13	0.99±0.11	2.43±0.10	3.89±0.15
<i>Down<sub>2</sub></i>	1.03±0.12	1.19±0.17	2.47±0.10	2.85±0.32
<i>Down<sub>3</sub></i>	1.24±0.13	0.89±0.10	1.52±0.11	4.60±0.37



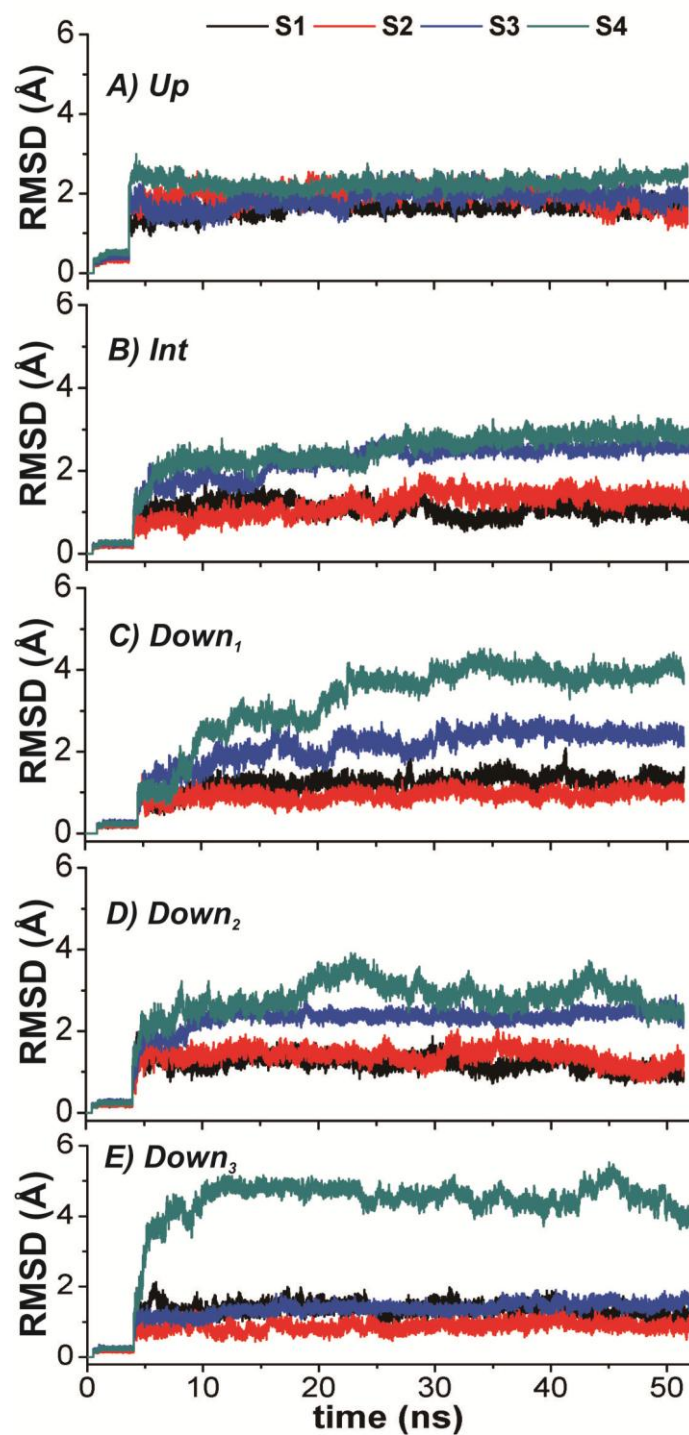


**Figure 3.9** RMSD of individual TM segment (S1-S4) of all five MD systems as a function of time.

### 3.5.2 Evidence of structure instability

RMSFs of all five simulations were computed by using the last 10-ns of the trajectories to assess conformational flexibility of the VSD with respect to the average structure. The range of RMSF magnitudes averaged over transmembrane residues was similar for all the simulated systems, as shown in Figure 3.10. The average backbone RMSF of S1, S2, S3 and S4 was summarized in Table 3.5. Due to helix-helix packing and helix-lipid interactions, residues in transmembrane helices exhibited lower RMSF values compared to those in N- and C-terminal ends, S1-S2 extracellular linker and S2-S3 intracellular linker. Nevertheless, a larger RMSF for residues near the C-terminal end of S3 and S4 was observed. This result is consistent with RMSD analysis and implies an existence of structure instability of the models.

**Table 3.5** The average RMSF for backbone atoms of transmembrane segments.

states	$\langle \text{RMSF} \rangle$ (Å)			
	S1	S2	S3	S4
<i>Up</i>	1.44	0.53	0.59	0.66
<i>Int.</i>	0.60	0.60	0.77	0.83
<i>Down<sub>1</sub></i>	0.85	0.76	0.95	0.88
<i>Down<sub>2</sub></i>	0.73	0.92	0.76	0.97
<i>Down<sub>3</sub></i>	0.63	0.61	0.65	1.12

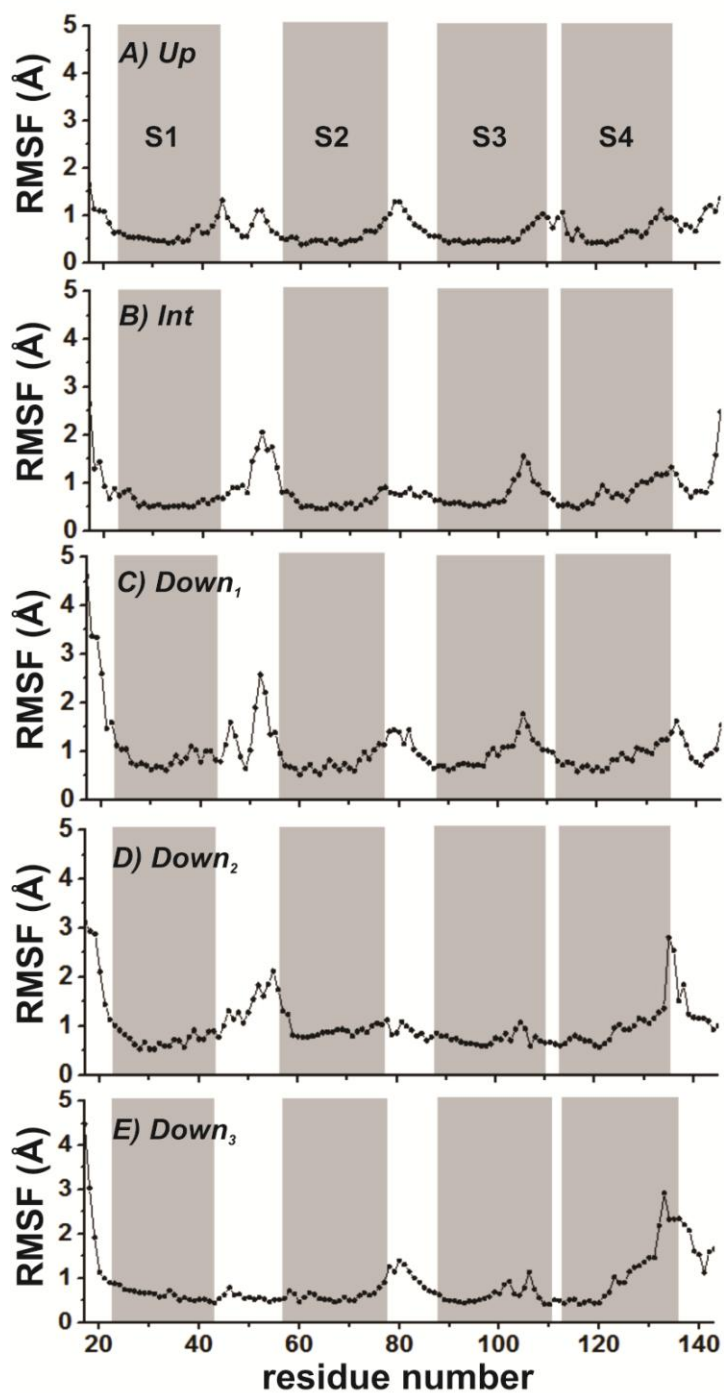


**Figure 3.10** Backbone RMSF values as a function of residue number of NaChBac-VSD computed using the last 10-ns of simulations. The transmembrane regions are indicated by striped background.

Stability secondary structure was analyzed by using the DSSP algorithm [54]. Overall profiles of secondary structure pattern show a major stability of  $\alpha$ -helical conformation, as shown in Figure 3.11. The S1, S2 and S3 are relatively stable compared to S4 which partially loses helicity for the C-terminal half of the segment. From the simulations, the transition from  $\alpha$ -helix to random coil was observed for the intracellular half of S4. There are a number of factors that affect structure instability of the model during the MD simulation. This includes types of phospholipids, position of protein in the membrane and quality of model itself. Nevertheless, an external force due to difference of membrane voltage also becomes a potentially important issue for the simulation of the resting state conformation of voltage-gated ion channel. At membrane potential = 0 mV, the voltage sensor domain is stabilized at the activated state whereas it undergoes conformational changes to the resting state at a negative membrane potential (about -70mV). In this study, the MD simulation of the intermediate and down states was performed in the absence of membrane voltage which is equivalent to 0 mV. This might be the case for the observation of secondary structure deformation of transmembrane voltage sensor.

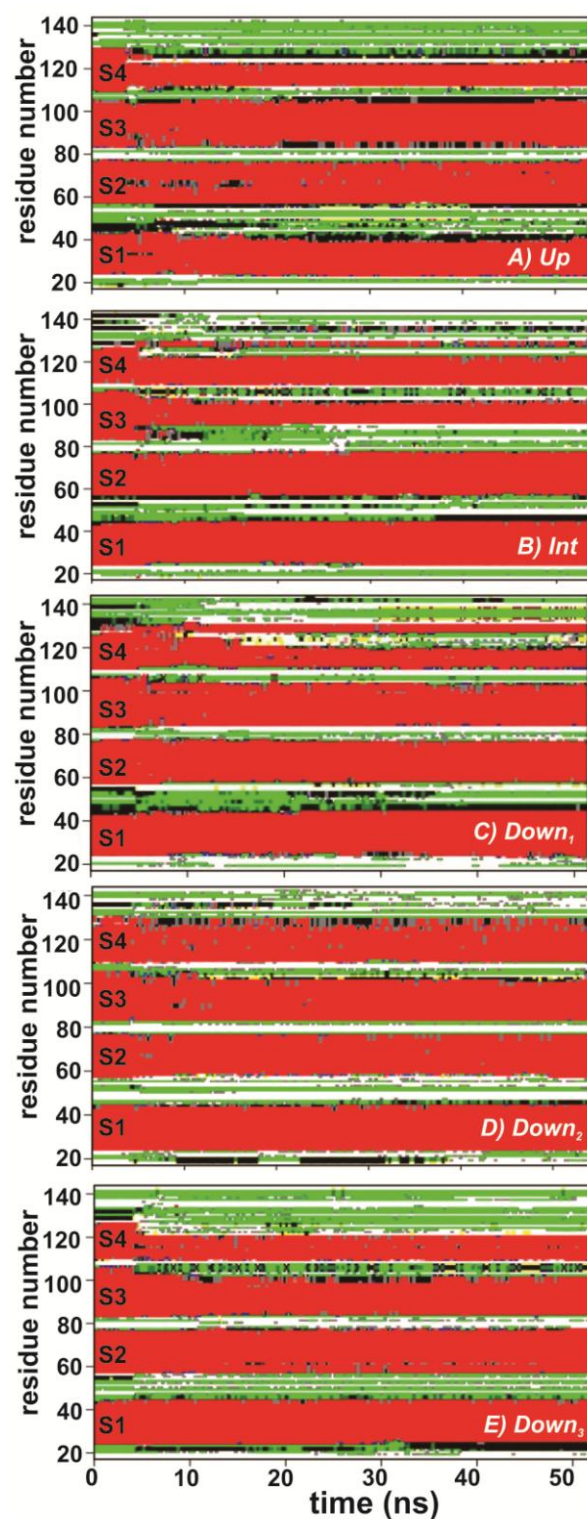


**Figure 3.11** Stability of secondary structure helices of the four TM segments as a function of simulation time calculated by DSSP. Each color means:  $\alpha$ -helix (red), stand in  $\beta$  sheet (blue),  $\beta$ -bridge (yellow),  $\beta$ -turn (black), coil (green), unassigned (white).

### 3.5.3 Salt bridge interactions

Although the S4 helix shows a partial deformation of secondary structure, useful information can be extracted from the MD simulations. Validity of the models was assessed by an analysis of salt bridge interactions involved with the S4 arginines. The interhelical salt bridges or hydrogen bonds involved with the four arginines of the voltage sensing segment were monitored from the simulations. The salt bridges, shown in Figure 3.12, comprises the interactions of R113 with E43 and D60, of R116 with D60, of R119 with D60 and D93, and the interactions of R122 with E70, D93 and S125 (BB stands for backbone atoms). From the simulation of the *Up* conformation, the salt bridges of R119 with D60 and of R122 with D93 were observed as shown in Figure 3.12. The R119-D60 interaction is in agreement with the experimental cross-link study. Analogous electrostatic interactions between S2, S3, and S4 have been proposed in *Shaker* K<sup>+</sup> channel. Further, the MD results showed that a hydrogen bond between the backbone of R122 and the hydroxyl group of S125 was being formed for the first 35 ns of the simulation, and then begun to disappear throughout the last 15 ns. This intrahelical hydrogen bond might play a role in the stability of secondary structure. In the *Int* model, the salt bridge of R119-D60 observed in the *Up* model was shifted to the pair between the second arginine R116 and D60, but that of R122-D93 was lost. In addition to the salt bridges, the intrahelical hydrogen bond of R122-S125 became more apparent in the *Int* model. It should be noted that a salt bridge between R119 and D93 was detected during the last 5 ns of simulation of the *Int* model.

Our MD simulations showed that all the three approximate models of the down configuration captured the important feature for the arginine-aspartic salt bridges. In the simulations, we monitored a putative salt bridge network involving E43, D60, R113 and R116. In all the down models, the pairs of charged residues R113-D60 form persistent salt bridge during the 50 ns time course of the simulations as shown in Figure 3.12. This suggested that the theoretical models satisfied the salt bridge interactions. An important difference between the models is the salt bridges of R116-D60 and R113-E43. The interactions between R113 and E43 were not observed in the simulation of *Down<sub>1</sub>*. For

*Down<sub>2</sub>*, the salt bridges of R116-D60 and R113-E43 were not retained throughout the 50 ns simulation. Only the simulation of *Down<sub>3</sub>* showed stable salt bridge network of the two outermost arginines with E43 of S1 and D60 of S2. The other two arginines, R119 and R122, of *Down<sub>1</sub>* and *Down<sub>3</sub>* form stable salt bridge interactions with D93 and E70, respectively, whilst those interactions were not present in *Down<sub>2</sub>*. Nevertheless, the backbone and positive charged sidechain of R122 in *Down<sub>2</sub>* were stabilized by hydrogen bond interaction with S125. The R122-S125 interactions were also detected for almost 45-ns of simulation of *Down<sub>3</sub>*.

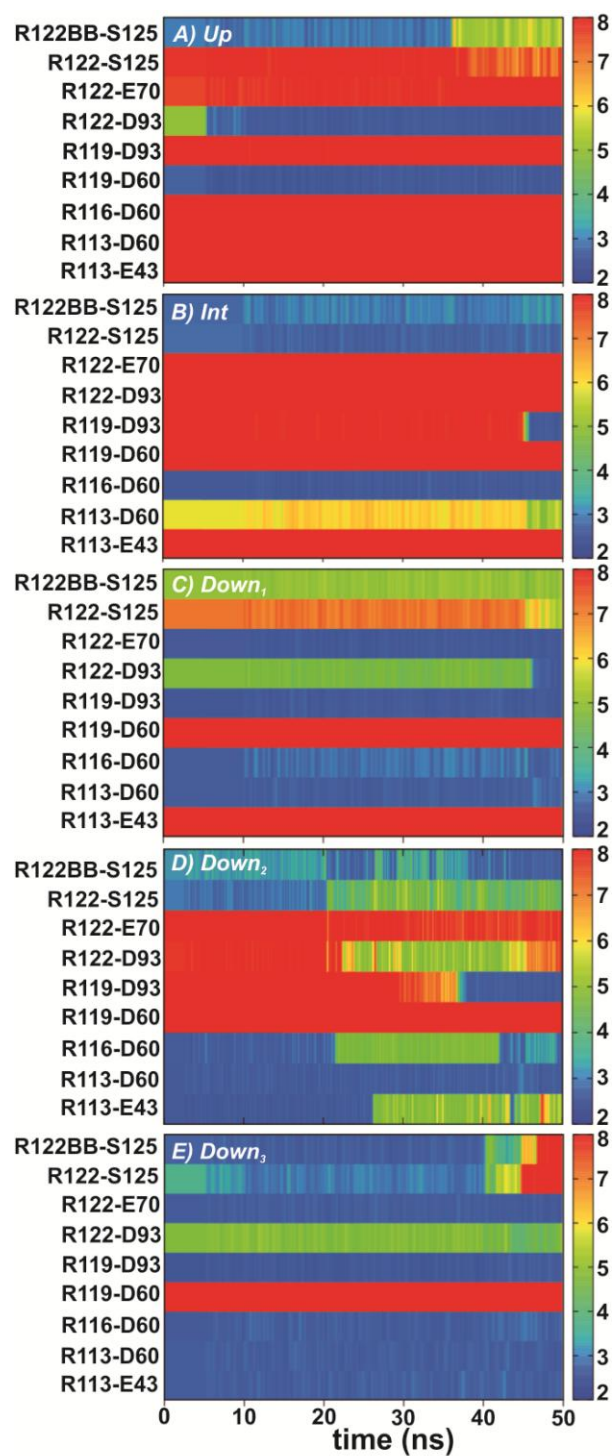


**Figure 3.12** The values of distances that represent key interactions in the four arginines of S4 of NaChBac-VSD. The distances are plotted on a color scale from blue (less than or equal to 2 Å) to red (greater than or equal to 8 Å).



### 3.5.4 Water-filled crevices in the VSD core

Deep crevices of both sides of the VSD cavity to which water can enter have been reported from the crystal structure of  $K_v$  channels. In addition, the presence of water-filled crevices in the VSD core was confirmed by accessibility measurement of sulfhydryl reagents to cysteine mutants of the channels [55]. From the simulations, the water density plot suggests that water molecules have diffused into the empty crevices of the VSD from both sides of the membrane bilayer. As illustrated in Figure 3.13 and 3.14, the transmembrane voltage sensor creates the hourglass shape water-filled crevices to house the gating charge-carrying arginines in the hydrophobic environment. However, water molecule cannot penetrate throughout the VSD pore. This was mainly due to the salt bridges which narrow the pathway and disrupted the passage of water. In the Up conformation, the salt bridge interactions between R119-D60 and R122-D93 prevent water molecules penetrating throughout the voltage sensor pore. Structure analysis of the MD trajectories indicated that R113 and R116 sidechains are near membrane interface and interact with waters and lipid head-groups whilst R119 and R122 sidechains are in hydrophobic region of the bilayer and interact with the negatively charged residues D60 and D93, as shown in Figure 3.12A. In the Int model, R113 and R122 sidechains interact with waters and lipid phosphate groups whereas R116 slips down toward the membrane. Hydrogen-bond networks of D60-R116-waters and D93-R119-waters were observed from the MD trajectory which therefore focuses the electric field to stabilize the positively charged S4 residues in a hydrophobic environment and reduces the energetic barrier to the S4 movement.

For the down states, R116 and R119 are distributed in the hydrophobic core where R113 and R122 are more accessible to lipid head groups and water. In particular, the most hydration of S1-S4 is observed for Down3. From the simulation, the four transmembrane segments are partially hydrated and water molecules associated with the protein in the bilayer. The hydrophobic thickness of the membrane is reduced by the protein hydration. It is expected that the water-filled crevices in the NaChBac-VSD focus the membrane electric field, which is in agreement with experimental and theoretical

studies. The insertion of water molecules have also been seen in the VSD of KvAP and Kv1.2 [56,57]. Consideration of the observed average water distributions in the presence of S1–S4 domains indicates that the membrane electric field drops over a distance of no more than about 25Å, the hydrophobic thickness of the bilayer in the presence of the voltage-sensing domain. Hydration of these critical residues will raise the local dielectric within the bilayer, ensuring that the arginine residues remain charged and thereby move in response to changes in membrane voltage.

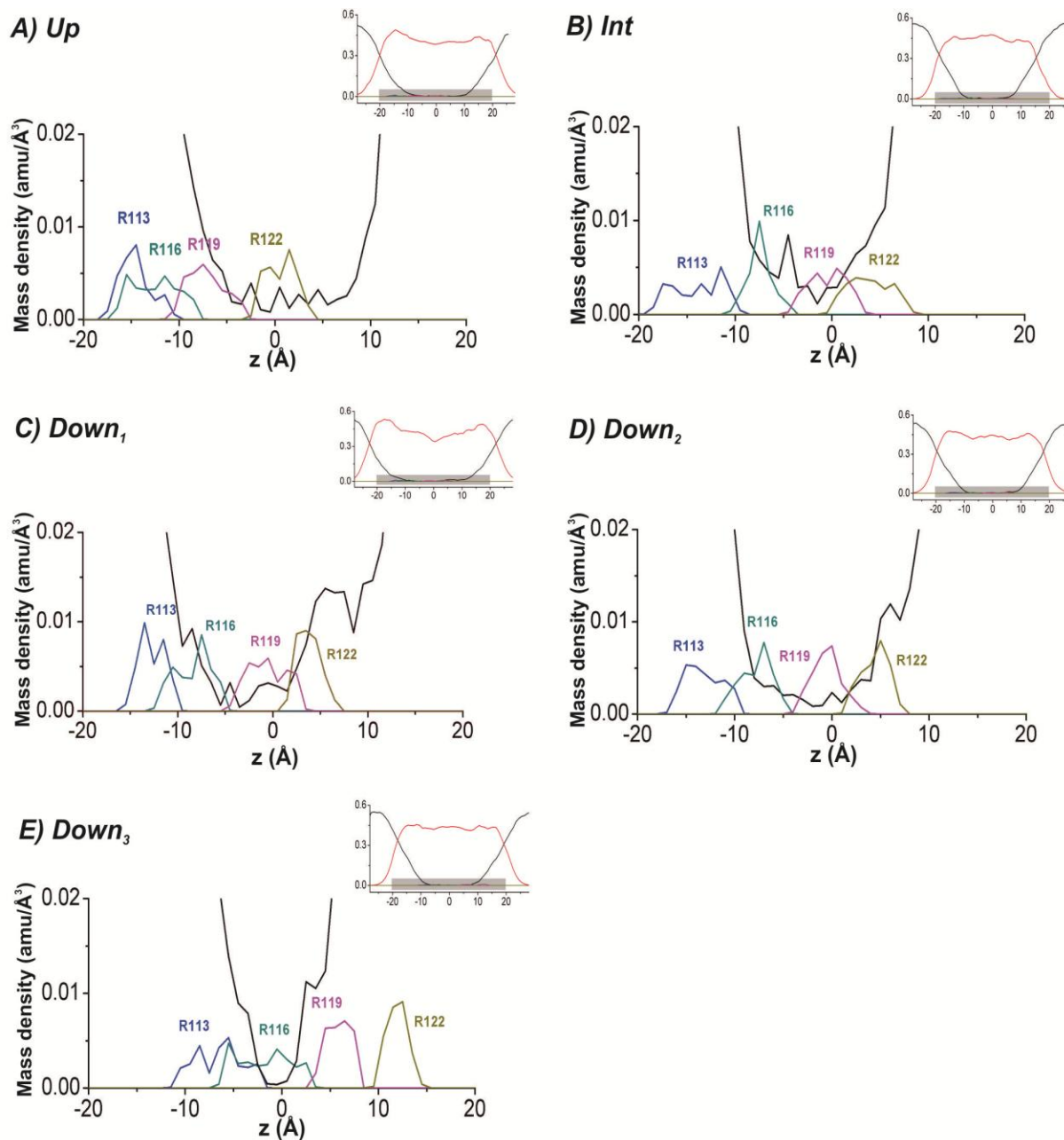


**Figure 3.13** Density profiles of water (black line) and the four arginines (R113 : blue, R116 : green, R119 : pink and R122 : yellow) in the simulations of the up, intermediate and down state. (Inset) the distribution of water (black line) and lipids (red line). The densities were average over the last 10 ns.

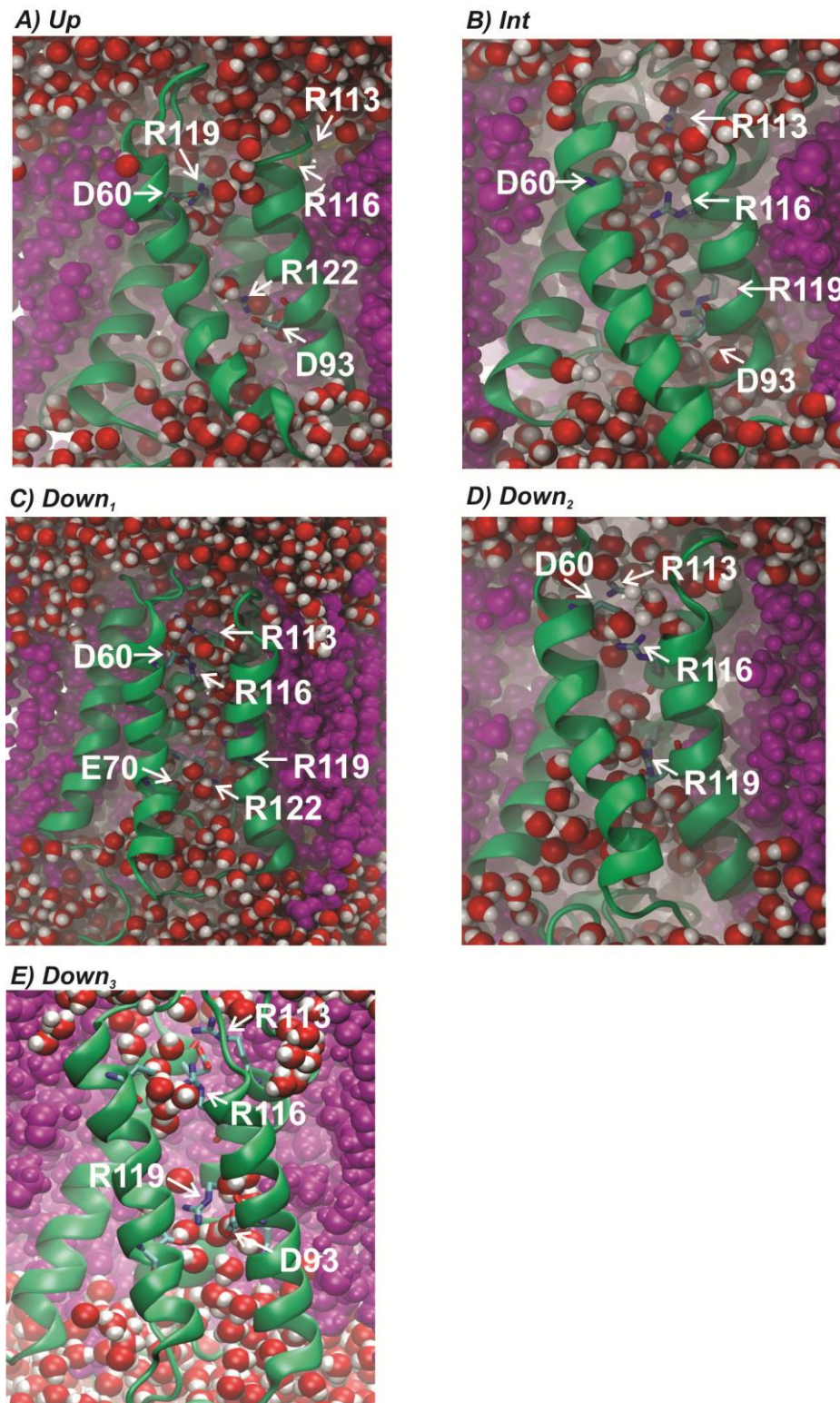


**Figure 3.14** Water – filled crevices in the VSD core.

### 3.5.5 Proposed transition model

Analysis of the MD results enables us to propose the putative transition models of gating charge arginines on the basis of changes in salt-bridge interactions as shown in Figure 3.15. In the up state, the R119 and R122 side chains form salt-bridge interactions with D60 of S2 and D93 of S3, respectively whereas R1 and R2 are surrounded by lipid phosphate head groups and water molecules. Upon membrane depolarization, the salt-bridges breaks and the S4 rotates and translates inward the bilayer. With a slight rearrangement of S1 during the S4 movement, salt bridges between positively charged residues on S4 and negatively charged residues on S1–S3 reform. One of a possibility is that because of the VSD motion a change of salt-bridge interactions from R119-D60 to R116-D60 is taken place as an intermediate. At the resting membrane potential, the S4 is continue to move until changes of salt-bridge interactions between the two outer most arginines with E43 of S1 and D60 of S2 are formed to stabilize the voltage sensor. Furthermore, R119 and R122 would involve the stability of the voltage sensor in the down state by salt-bridge formations with E70 and D93, respectively. The results observed from the MD simulations are in good agreement with structural and functional studies.

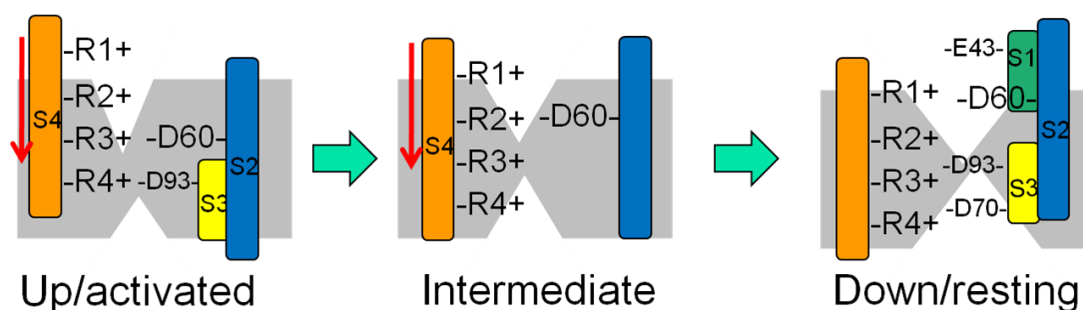


**Figure 3.15** The proposed transmittion of “up”, “int” and “down” states of NaChBac – VSD

## CHAPTER IV

### CONCLUSION

In the present study, putative activated (Up) and resting (Down) conformations of transmembrane voltage sensor domain from NaChBac channel were developed based on biophysical and biochemical data. The structure and dynamic properties were extracted from the 50ns MD simulations of the Up, the intermediate and the three Down models in the presence of hydrated phospholipid bilayer. From the MD results, the transmembrane structure of the Up state is more stable than that of the intermediate and Down states. The observed structure instability, especially the S4 segment, is likely to be associated with the protein-membrane system simulated without incorporating the negative membrane potential which has shown to stimulate the closed channel with the VSD in the Down state. Nevertheless, the results of the simulations provide useful information for a general motion of the voltage sensing segment in a context of helical screw mechanism. This was demonstrated by the Up and Down models showing a counter charge exchange of the S4 arginines. In the Up model, the salt-bridge interactions between R3 and D60 are stable during the course of MD simulation whilst the R1 and R2 face outside the VSD core, making its sidechain exposed to water and lipid phosphate groups. However, all the putative Down and intermediate models show changes of R1, R2 and R3's surrounding environment where R1 and R2's sidechains potentially form salt-bridges with E43 of S1 and D60 of S2. A tendency of R3's sidechain forming a counter charge interaction with D93 was observed in the Down state model. The results are in good agreement with electrophysiology data of NaChBac mutants. An estimated distance of the S4 movement from the Up to the Down models is about 3-5 Å which is equivalent to one helical turn. As the S4 moves downward, structure rearrangement of transmembrane S1, S2 and S3 segments were observed. As a result, the water-filled crevice expands, allowing water molecules more accessible to the inner cavity of VSD core. The results supported the predicted changes of sulfhydryl accessibility to the voltage sensor domain of the NaChBac channel in the resting state.

However, there are questions that remained unanswered from the present study. This includes the number of gating charge, the effect of the increased hydrophilicity in the VSD inner cavity or free energy of conformational transition etc. It is important to note that all the interpretations of the study are relied on the model developed based on the crystal structure of Kv channels. Although structure comparison between NaChBac-VSD and the new x-ray NavAb-VSD revealed closed similarity of overall transmembrane orientation, a remodeling of NaChBac-VSD structures will give useful information and confident interpretation.

## REFERENCES

- [1] Hille, B. Ion channels of excitable membranes (3rd ed.). Sunderland, Mass: Sinauer Associates. ISBN 0-87893-321-2.
- [2] William, A. C. Ion channel voltage sensors: structure, function, and Pathophysiology. Neuron 67 (2006) : 915-928.
- [3] Hodgkin, A., Huxley A. A quantitative description of membrane current and its application to conduction and excitation in nerve. Journal of Physiology 117 (1952) : 500-544.
- [4] Frank, H.Y., Vladimir, Y.Y., George, A.G., William, A.C. Overview of molecular relationships in the voltage-gated ion channel superfamily. Pharmacological Reviews 57 (2005) : 387-395.
- [5] Armstrong, C.M., Hille, B. Voltage-gated ion channels and electrical excitability. Neuron 20 (1998) : 371-380.
- [6] Liu, Y., Holmgren, M., Jurman, M.E., Yellen, G. Gated access to the pore of a voltage-dependent K<sup>+</sup> channel. Neuron 19 (1997) : 175-184.
- [7] Sands, Z., Grottesi, A., Sansom, M.S. Voltage-gated ion channels. Current Biology 15 (2005) : 44-47.
- [8] Unwin, N. Neurotransmitter action: opening of ligand-gated ion channels. Neuron 10 (1993) : 31-41.
- [9] Keramidas, A., Moorhouse, A.J., Schofield, P.R., Barry, P.H. Ligand-gated ion channels: mechanisms underlying ion selectivity. Progress in Biophysics and Molecular Biology 86 (2004) : 161-204.
- [10] Martinac, B. Mechanosensitive ion channels: molecules of mechanotransduction. Journal of Cell Science 117 (2004) : 2449-2460.
- [11] Azimen, L. Ion channel function. [Online]. 2009. Available from : <https://wiki.brown.edu/confluence/display/Spring07BN0102S01/Ion+Channel+Function> (2009, February 01)
- [12] Fraser, S.P., Pardo, L.A. Ion channels: functional expression and therapeutic



- potential in cancer. EMBO Reports 9 (2008) : 512-515.
- [13] Chanda, B., Bezanilla, F. A common pathway for charge transport through voltage-sensing domains. Neuron 57 (2008) : 345-351.
- [14] Bezanilla, F. Voltage-gated ion channels. IEEE Transactions on Nanobioscience 4 (2005) : 34-48.
- [15] Treptow, W., Klein, M.L. Computer simulations of voltage-gated cation channels. Journal of Physical Chemistry Letters 3 (2012) : 1012-1023.
- [16] Den, L. Action potential (nerve impulse). [Online]. 2009. Available from : <http://pesbiology.blogspot.com/2009/11/new-material-review.html> (2009, November 11)
- [17] Numa, S., Noda, M. Molecular structure of sodium channels. Annals of the New York Academy of Sciences 479 (1986) : 338-355.
- [18] Borjesson, S.I., Elinder, F. Structure, function, and modification of the voltage sensor in voltage-gated ion channels. Cell Biochemistry and Biophysics 52 (2008) : 149-174.
- [19] Dong, K. Insect sodium channels and insecticide resistance. Invertebrate Neuroscience Journal 7 (2007) : 17-30.
- [20] Pavlov, E., Bladen, C., Winkfein, R., Diao, C., Dhaliwal, P., French, R. The pore, not cytoplasmic domains, underlines inactivation in a prokaryotic sodium channel. Journal of Biophysical 89 (2005) : 232-241.
- [21] Navarro, B., Kirichock, Y., Chung, J. J., Clapham, D. E. Ion channels that control fertility in mammalian spermatozoa. International Journal of Developmental Biology 52 (2008) : 607-613.
- [22] Marban, E., Yamagishi, T., Tomaselli, G. F. Structure and function of voltage-gated sodium channels. Journal of Physiology 508 (1998) : 647-657.
- [23] Frank, H. Y., William, A. C. Overview of the voltage-gated sodium channel family. Genome Biology 4 (2003) : 207-213.
- [24] Bezanilla, F. The voltage sensor in voltage-dependent ion channels. Journal of Physiology 80 (2000) : 555-592.

- [25] Swartz, K. J. Sensing voltage across lipid membranes. Nature 456 (2008) : 892-897.
- [26] Barnett, M. W., Larkman, P. M., The action potential. Practice Neurology 7 (2007) : 192-197.
- [27] Lai, H. C., Jan, L. Y. The distribution and targeting of neuronal voltage-gated ion channels. Nature 7 (2006) : 548-562.
- [28] Ren, D., Navarro, B., Xu, H., Yue, L., Shi, Q., Clapham, D. E. A prokaryotic voltage-gated sodium channel. Science 294 (2001) : 2372-2375.
- [29] Chahine, M., Pilote, S., Pouliot, V., Takami, H., Sato, C. Role of arginine residues on the S4 segment of the *Bacillus halodurans* Na<sup>+</sup> channel in voltage-sensing. Journal of Membrane Biology 201 (2004) : 9-24.
- [30] Shimomura, T., Irie, K., Nagura, H., Imai, T., Fujiyoshi, Y. Arrangement and mobility of the voltage sensor domain in prokaryotic voltage-gated sodium channel. The Journal of Biological Chemistry 286 (2011) : 7409-7417.
- [31] Charalambous, K., Wallace, B. A. NaChBac: The long lost sodium channel ancestor. Journal of the American Chemical Society 50 (2011) : 6742-6752.
- [32] Blanchet, J., Pilote, S., Chahine, M. Acidic residues on the voltage-sensor domain determine the activation of NaChBac sodium channel. Journal of Biophysical 92 (2007) : 3513-3523.
- [33] Yang, N., Horn, R. Evidence for voltage-dependent S4 movement in sodium channels. Neuron 15 (1995) : 213-218.
- [34] Yue, L., Navarro, B., Ren, D., Ramos, A., Clapham, D. E. The cation selectivity filter of the bacterial sodium channel, NaChBac. Journal of Cell Biology 120 (2002) : 845-853.
- [35] Jiang, Y., Lee, A., Chen, J., Ruta, V., Cadene, M., Chait, B. T., Mackinnon, R. X-ray structure of a voltage-dependent K<sup>+</sup> channel. Nature 423 (2003) : 423, 33-41.
- [36] Murata, Y., Iwasaki, H., Sasaki, M., Inaba, K., Okamura, Y. Phosphoinositide phosphatase activity coupled to an intrinsic voltage sensor. Nature 435 (2005) : 1239-1243.
- [37] Ramsey, S., Moran, M. M., Chong, J. A., Clapham, D. E. A voltage-gated proton-

- selective channel lacking the pore domain. Nature 440 (2006) : 1213-1216.
- [38] Durell, S. R., Guy, H.R. Atomic scale structure and functional models of voltage-gated potassium channels. Journal of Biophysical 62 (1992) : 238-247.
- [39] Sigworth, F. Voltage gating of ion channels. Quarterly Review of Biophysics 27 (1993) : 1-40.
- [40] Rizvi, S.H., Shoeb, A., Kapil, R.S., Popli, S.P. Two diuretic triterpenoids from *Antidesma menasu*. Phytochemistry 19 (1980) : 2409-2410.
- [41] Tombola, F., Pathak, M. M., Isacoff, E. Y. How does voltage open an ion channel? Annual Review of Cell and Developmental Biology 22 (2006) : 23-52.
- [42] Horn, R. How ion channels sense membrane potential. Proceedings of the National Academy of Sciences 102 (2005) : 4929-4930.
- [43] Chakrapani, S., Sompornpisut, P., Intrarathep, P., Roux, B., Perozo, E. The activated state of a sodium channel voltage sensor in a membrane environment. Proceedings of the National Academy of Sciences 107 (2010) : 5435-5440.
- [44] Paldi, T., Gurevitz, M. Coupling between residues on S4 and S1 defines the voltage-sensor resting conformation in NaChBac. Journal of Physicals 90 (2010) : 456-463.
- [45] Phillips, J. C., Braun, R., Wang, W., Gumbat, J., Tajkhorshid, E., Villa, E., Chipot, C., Skeel, R. D., Kale, L., Schulten, K. Scalable molecular dynamic with NAMD. Journal of Computational Chemistry 26 (2005) : 1781-1802.
- [46] Callenberg, K. M., Choudhary, O. P., Forest, G. L., Gohara, D. W., Baker, N. A., Grabe, M. APBSmem: A graphical interface for electrostatic calculations at the membrane. Public Library of Science 5 (2010) : 12722-12732.
- [47] Sompornpisut, P., Roux, B., Perozo, E. Structural refinement of membrane proteins by restrained molecular dynamics and solvent accessibility data. Journal of Biophysicals 95 (2008) : 5349-5361.
- [48] Nina, M., Beglov, D., Roux, B. Atomic radii for continuum electrostatics calculations based on molecular dynamics free energy simulations. The Journal of Physical Chemistry B 101 (1997) : 5239-5248.

- [49] Baker, N, MaCammon, J. A., Holst, M. Adaptive Poisson-Boltzmann solver. [Online]. 2010. Available from : <http://www.poissonboltzmann.org> (2010, October 10)
- [50] Hinchliffe, A. Modelling molecular structures. John Wiley & Sons 2000, ISBN 10: 0-47195-923-5.
- [51] Long, S. B., Tao, X., Campbell, E. B., MacKinnon, R. Atomic structure of a voltage-dependent  $K^+$  channel in a lipid membrane-like environment. Nature 450 (2007) : 376-382.
- [52] Payandeh, J., Scheuer, T., Zheng, N., Catterall, W. A. The crystal structure of a voltage-gated sodium channel. Nature. 475 (2011) : 353-358.
- [53] Grabe, M., Lecar, H., Jan, N. Y., Jan, Y.L. A quantitative assessment of models for voltage-dependent gating of ion channels. Proceedings of the National Academy of Sciences 101 (2004) : 17640-17645.
- [54] Kabsch, W., Sander, C. Dictionary of protein secondary structure: pattern recognition of hydrogen-bonded and geometrical features. Biodegradable and Biobased Polymers 22 (1983) : 2577-2637.
- [55] Nguyen, T. P., Horn, R. Movement and crevices around a sodium channel S3 segment. The Journal of General Physiology 120 (2002) : 419-436.
- [56] Treptow, W., Tarek, M. Environment of the gating charges in the Kv1.2 shaker potassium channel. Journal of Biophysics 90 (2006) : 64-66.
- [57] Freites, J. A., Tobias D. J., White, S. H. A voltage-sensor water pore. Journal of Biophysics 91 (2006) : 90-92.

## **APPENDIX**

**Programming A.1** Analysis script backbone RMSD.

```

set initmol [mol load psf ../../02membrane/nabach_dwn_popcwi.psf      pdb
../../02membrane/nabach_dwn_popcwi.pdb]
set outfile [open rmsd_alpha01-16.dat w]
set frame0 [atomselect $initmol "protein and alpha and noh" frame 0]

set trajmol [mol load psf ../../02membrane/nabach_dwn_popcwi.psf      dcd
../dcd/dcd/nabach_popcwi-01-relaxtail.dcd]
mol addfile ../dcd/dcd/nabach_popcwi-02-fixprot.dcd type dcd first 0 last -1 waitfor all
mol addfile ../dcd/dcd/nabach_popcwi-03eq.dcd type dcd first 0 last -1 waitfor all
mol addfile ../dcd/dcd/nabach_popcwi-04.dcd type dcd first 0 last -1 waitfor all
mol addfile ../dcd/dcd/nabach_popcwi-05.dcd type dcd first 0 last -1 waitfor all
mol addfile ../dcd/dcd/nabach_popcwi-06.dcd type dcd first 0 last -1 waitfor all
mol addfile ../dcd/dcd/nabach_popcwi-07.dcd type dcd first 0 last -1 waitfor all
mol addfile ../dcd/dcd/nabach_popcwi-08.dcd type dcd first 0 last -1 waitfor all
mol addfile ../dcd/dcd/nabach_popcwi-09.dcd type dcd first 0 last -1 waitfor all
mol addfile ../dcd/dcd/nabach_popcwi-10.dcd type dcd first 0 last -1 waitfor all
mol addfile ../dcd/dcd/nabach_popcwi-11.dcd type dcd first 0 last -1 waitfor all
mol addfile ../dcd/dcd/nabach_popcwi-12.dcd type dcd first 0 last -1 waitfor all
mol addfile ../dcd/dcd/nabach_popcwi-13.dcd type dcd first 0 last -1 waitfor all
mol addfile ../dcd/dcd/nabach_popcwi-14.dcd type dcd first 0 last -1 waitfor all
mol addfile ../dcd/dcd/nabach_popcwi-15.dcd type dcd first 0 last -1 waitfor all
mol addfile ../dcd/dcd/nabach_popcwi-16.dcd type dcd first 0 last -1 waitfor all
set nf [molinfo $trajmol get numframes]
set sel [atomselect $trajmol "protein and alpha and noh"]
# rmsd calculation loop
for {set i 1} {$i < $nf} {incr i} {
    $sel frame $i

```

```

$sel move [measure fit $sel $frame0]
set time [expr ($i * 2.) / (1000.) ]
# puts "$time [measure rmsd $sel $frame0]"
puts $outfile "$time [measure rmsd $sel $frame0] $i"
# puts $outfile "$i [measure rmsd $sel $frame0]"
}
close $outfile
exit

```

### **Programming A.2** Analysis script RMSF of individual TM segment

```

mol load psf ../../../../02membrane/nabach_dwn_popcwi.psf dcd ../nabach_popcwi-12.dcd
foreach no { 13 14 15 16 } {
mol addfile ../nabach_popcwi-$no.dcd type dcd first 0 last -1 waitfor all
}

```

```

set reference [atomselect top "protein and backbone" frame 0]
set compare [atomselect top "protein and backbone"]
set all [atomselect top "all"]
set num_steps [molinfo top get numframes]
puts $num_steps

for {set frame 0} {$frame < $num_steps} {incr frame} {
$compare frame $frame
set trans_mat [measure fit $compare $reference]
$all frame $frame
$all move $trans_mat
}
set outfile [open rmsf_model1.dat w]
set nf [molinfo top get numframes]

```

```
set sel [atomselect top "name CA"]
set rmsf [measure rmsf $sel first 1 last [expr {$nf-1}] step 1]

for {set i 0} {$i < [$sel num]} {incr i} {
  puts $outfile "[expr {$i+17}] [lindex $rmsf $i]"
}
exit
```



# ELECTROSTATIC SOLVATION FREE ENERGY OF Na<sub>v</sub> AND K<sub>v</sub> VOLTAGE SENSOR IN MEMBRANE BY POISSON-BOLTZMANN SOLVENT CONTINUUM METHOD

Wannaruedee Wannapukdee<sup>1</sup> and Pornthep Sompornpisut<sup>1,\*</sup>

<sup>1</sup>Computational Chemistry Unit Cell, Department of Chemistry, Faculty of Science,  
Chulalongkorn University, Bangkok 10330, Thailand

\* Author for correspondence: E-Mail: spornthe@hotmail.com, Tel. +662-2187604

**Abstract:** Electrostatic forces play an important role in protein stability, solvation, folding and function. Voltage sensor domain (VSD) of voltage-dependent ion channels has shown to be a functional independence module in a variety of voltage-activated ion channels and enzymes. VSD consisting of four transmembrane segments, of which the S4 segment containing many positively charged arginines is crucial for the voltage sensitivity. In this study, we examined the energy required to transfer the transmembrane voltage sensor from high dielectric aqueous-like media into low dielectric membrane-like solvent. Poisson-Boltzmann continuum electrostatic method was employed to compute electrostatic solvation energy of the VSD in KvAP, Kv1.2-2.1, NavAb, and NaChBac. The results showed the solvation energy follow the order Kv1.2-2.1 < NaChBac < NavAb < KvAP. Per residue decomposition energy analysis revealed that the charged arginines on S4 exhibit typical high value of electrostatic solvation free energy which are common to all Na<sub>v</sub> and K<sub>v</sub>.

## 1. Introduction

Voltage-gated sodium (Na<sub>v</sub>) and potassium (K<sub>v</sub>) channels are integral membrane proteins that control, an influx of sodium ions and an efflux of potassium ions through plasma membrane [1-4], respectively. They are responsible for generation and propagation of action potential in neurons and other excitable cells. Both Na<sub>v</sub> and K<sub>v</sub> open and close the channel gate in response to changes of membrane voltage. Generally, Na<sub>v</sub> and K<sub>v</sub> are composed of four homologous domains with membrane spanning  $\alpha$ -helices. Each domain consists of six transmembrane segments (S1-S6). The Na<sub>v</sub> and K<sub>v</sub> voltage sensors are composed of the first four transmembrane helices, S1-S4, packed counterclockwise and formed voltage sensor domain (VSD). In particular, the S4 acts as the voltage-sensing segment as it contains four to eight positively charged and highly conserved arginine residues.

Considerable efforts have been made to understand the structure basis associated with the voltage-dependent mechanism of VSD by both experimental and computational studies [5-8] because it has shown to be a functional independence module in a variety of voltage-activated ion channels and enzymes. From our previous study [8], a structural model of the VSD from *Bacillus halodurans* Na channel (NaChBac) in the activated or "up" state conformation has been derived

from site-directed spin-labeling and EPR solvent accessibility data.

In this study, we wanted to further explore the energetic aspects of our model embedded in membrane environments. Especially, we computed the energetic cost associated with an insertion of VSD in lipid bilayer. Although the transmembrane segments of the VSD are largely composed of hydrophobic residues, the S4 segment is rich of positively charged residues. The unfavorable solvation energy associated with the exposure of the S4 segment to the membrane is the issue of basis fundamental interest. The implicit solvent with continuum Poisson-Boltzmann (PB) based approach was employed to calculate the electrostatic components of free energy of solvation required to transfer the transmembrane voltage sensor from aqueous media into membrane bilayer. For comparison, the electrostatic solvation energy calculations were carried out for the voltage sensor of KvAP, Kv1.2-2.1 and NavAb whose the 3D x-ray structures are available [9-11].

## 2. Methods

The electrostatic calculation in this study is on the basis of solving the PB equation. The Poisson equation representing the reversible work of charging the solute can be given as

$$\nabla \cdot \epsilon(\vec{r}) \nabla \Phi(\vec{r}) = -\rho(\vec{r}),$$

where  $\epsilon$  is the dielectric constant,  $\Phi$  is the electrostatic potential, and  $\rho$  is the charge density, i.e. all atomic charges within the solute. All three variables are position-dependent functions represented by the position vector  $r$ . By considering the solute dissolved in electrolyte solution, the Poisson-Boltzmann equation (PBE) was used instead of the Poisson equation where  $\phi = e\Phi/k_B T$  is the reduced electrostatic potential.

$$-\nabla \cdot [\epsilon(\vec{r}) \nabla \phi(\vec{r})] + \bar{\kappa}^2(\vec{r}) \sinh[\phi(\vec{r})] = -\frac{e}{k_B T} 4\pi\rho(\vec{r}),$$

,  $\bar{\kappa}^2$  is the Debye-Hückel screening parameter, which accounts for ionic shielding. For a given protein configuration and dielectric constants of solute environment,  $\Phi$  can be obtained and the total

electrostatic energy is determined the sum over all charges in the system

$$\Delta G_{elec} = \sum \Phi(\vec{r})\rho(\vec{r}),$$

To examine the electrostatic free energy accounting for the insertion of transmembrane segments to lipid bilayer,  $\Delta G_{elec}$  was computed for  $K_v$  and  $Na_v$  voltage sensors immersed implicitly in different solvents (Fig. 1). The electrostatic solvation free energy of the voltage sensors in bulk water,  $\Delta G_{elec,water}$ , was obtained by employing a continuum solvent model treating with high dielectric aqueous-like media. For calculating the solvation energy of the voltage sensors in membrane environments,  $\Delta G_{elec,membrane}$ , a planar low-dielectric slab was introduced to PB method as water inaccessible region. The energy change upon transferring the VSD from bulk water to membrane bilayer was obtained by subtracting the solvation energy of the protein in lipid from that in bulk water as follow:

$$\Delta G_{elec} = \Delta G_{elec,membrane} - \Delta G_{elec,water}$$

The calculations were performed by using the program Adaptive Poisson-Boltzmann Solver (APBS) 1.2.1 [12] with help of a java-based graphical user interface APBSmem for setting up input parameters [13]. 3D structure coordinates of VSD of KvAP (1ORS), Kv1.2-2.1 (2R9R) and NavAb (3RVY) were taken Protein Data Bank, whereas NaChBac-VSD was obtained from our previous study [8]. To construct the model systems, the Kv1.2-2.1 channel was oriented to align the pore along the z-axis to give a proper orientation of the voltage sensor with respect to the bilayer normal. Then we selected only one chain of the oriented VSD and performed a translation on the xy-plane to move the center of mass of the VSD to the z-axis. The orientation of KvAP, NavAb and NaChBac voltage sensor in the membrane were a result of superimposition method using sequence and structure alignment of the conserved S1 and S2 segments of the oriented VSD of Kv1.2-2.1. Transformation of atomic coordinates were done using VMD and command scripts[13]. The program PDB2PQR was used to add hydrogen atoms together with assign atomic charges and radii [12]. Partial atomic charges and radii of the protein were taken from the CHARMM22 parameter sets. The sequential focusing multigrid algorithm in solving PBE consists of three resolution maps:  $300 \times 300 \times 300 \text{ \AA}^3$  for coarse,  $200 \times 200 \times 200 \text{ \AA}^3$  for medium, and  $100 \times 100 \times 100 \text{ \AA}^3$  for fine resolutions. Grid points of  $161 \times 161 \times 161$  were employed to all maps. The implicit membrane slab was introduced such that its plane is in the Cartesian xy-plane and the bilayer normal is aligned along the z-axis. A thickness of membrane bilayer ( $L_{mem}$ ) was evaluated between 30-40  $\text{\AA}$ . The dielectric constants for the membrane ( $\epsilon_m$ ) and water ( $\epsilon_w$ ) was 2 and 80, respectively. The dielectric constant of protein was varied between 2, 4 and 10. Ionic strength was 0.1 M with coulomb charge

+1 and -1, and radius 2.0  $\text{\AA}$ . Water probe radius was 1.4  $\text{\AA}$ .

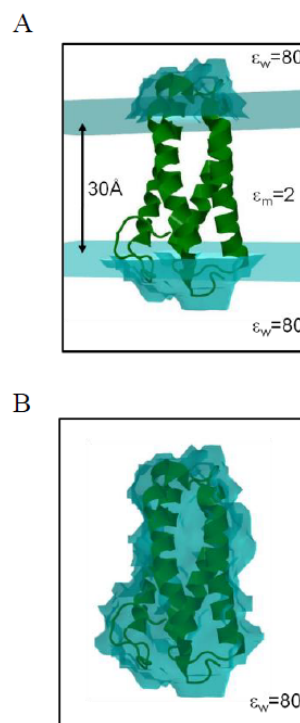


Figure 1. Model systems used to compute electrostatic free energy of protein solvation. (A) The VSD is embedded in the membrane. The membrane region between the two blue planes is assigned a dielectric value  $\epsilon_m = 2$ . Bulk water above and below the membrane is assigned a dielectric value of  $\epsilon_w = 80$ . (B) The VSD in the bulk water ( $\epsilon_w = 80$ ) without the membrane. The protein solvation energy is calculated by  $\Delta G_{elec} = \Delta G_A - \Delta G_B$ .

### 3. Results and Discussion

#### 3.1 Electrostatic solvation energy of NaChBac-VSD as a function of $\epsilon$ and membrane thickness

Electrostatic free energies of protein solvation were calculated for the voltage sensor domain of NaChBac, KvAP, Kv1.2-2.1 and NavAb. The results show that all protein solvation energies are positive. This indicates that for a spontaneous change the protein needs the energy to do work. In other words, the insertion of VSD from bulk water to the membrane needs an external driving force. As shown in Table 1, an increase of membrane thickness results in an increase of the protein solvation energies. However, the solvation energies decrease upon an increase of protein dielectric

Table 1. Electrostatic solvation energies of NaChBac-VSD as a function of  $\epsilon$  and membrane thickness ( $L_{\text{mem}}$ )

$\epsilon_{\text{protein}}$	$L_{\text{mem}}$ (Å)	$\Delta G_{\text{elec}}$ (kcal/mol)
2	30	136.2
2	35	195.0
2	40	296.4
4	30	91.5
4	35	134.3
4	40	201.7
10	30	48.5
10	35	72.2
10	40	114.0

### 3.2 Solvation energies of $K_v$ and $Na_v$ voltage sensors

The solvation energies of the  $K_v$  and  $Na_v$  voltage sensors (Table 2) follow the order:  $Kv1.2-2.1 < NaChBac < NavAb < KvAP$ . The solvation energy was decomposed into partial contribution of each residue. Apparently, the energies were mainly contributed from the solvation of transmembrane residues rather than that of non-transmembrane residues (Fig.2). Particularly, the S4 segment of  $K_v$  and  $Na_v$  contributes significantly to the solvation energy.

Table 2. Electrostatic solvation energies of  $K_v$  and  $Na_v$  voltage sensors ( $\epsilon_{\text{protein}} = 4$ ,  $L_{\text{mem}} = 30$  Å)

Type	$\Delta G_{\text{elec}}$ (kcal/mol)
KvAP	231.6
Kv1.2-2.1	85.1
NavAb	150.1
NaChBac	91.5
S4 (KvAP)	472.2-458.9 [14]

The solvation free energies of four highly conserved arginines on the S4 segment were shown in Table 3. Based on sequence alignment of voltage-gated ion channel homolog, R1, R2, R3 and R4 are used to define the sequential position of arginines on the S4 segment. Arginines that contribute substantially to the solvation free energy include R1, R2 and R4 of KvAP, R2 and R3 of NavAb, and R4 of NaChBac. It appears that these arginines are either highly exposed to the solvent environment or not form salt-bridge interactions with the negative charge residues.

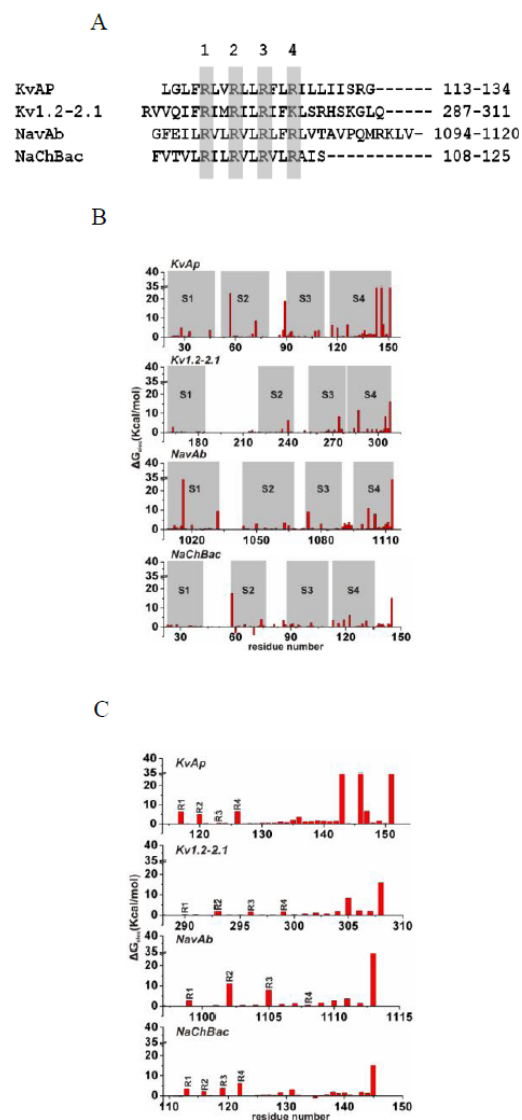


Figure 2. Per-residue contribution to the solvation energy (A) sequence alignment of the S4 segment, (B) residues on the S4 segment and (C) all residues of voltage sensor domain.

Table 3. Electrostatic solvation energies of the S4 arginines

Type	$\Delta G_{\text{elec}}$ (kcal/mol)			
	R1	R2	R3	R4
KvAP	6.5	5	0.5	6.5
Kv1.2-2.1	0.4	2	1.2	1.2
NavAb	2.5	11	8	0.9
NaChBac	3.2	2	3.3	6

#### 4. Conclusions

We evaluated the electrostatic free energy of solvation of the known 3D structures of Na<sub>v</sub> and K<sub>v</sub> voltage sensor in membrane using Poisson-Boltzmann continuum dielectric models. The results showed the external driving force is needed to transfer the voltage sensor domain from bulk water into the membrane. The solvation energy of KvAP appears to be the greatest. Per-residue decomposition energy analysis revealed that most of the charged arginines on S4 contribute significantly to the solvation energy.

#### Acknowledgements

This work is supported by the National Research University Project of CHE, Ratchadaphiseksomphot Endowment Fund (HR1155A) and the Thai Government Stimulus Package 2 (TKK2555) under the Project for Establishment of Comprehensive Center for Innovative Food, Health Products and Agriculture. The Center of Excellence for Petroleum, Petrochemicals and Advanced Materials, Chulalongkorn University.

#### References

- [1] Numa, S.; Noda, M. Molecular structure of sodium channels. *Am. N. Y. Acad. Sci.* **1986**, *479*, 338-355.
- [2] Ren, D.; Navarro, B.; Xu, H.; Yue, L.; Shi, Q.; Clapham, D. E. A Prokaryotic voltage-gated sodium channel. *Science* **2001**, *294*, 2372-2375.
- [3] Doyle, D. A.; Cabral, J. M.; Pfuetzner, R. A.; Kuo, A.; Gulbis, J. M.; Cohen, S. L.; Chait, B. T.; MacKinnon, R. The structure of the potassium channel: molecular basis of K<sup>+</sup> conduction and selectivity. *Science* **1998**, *280*, 69-77.
- [4] Han, M.; Zhang, J. Z. H. Molecular dynamic simulation of the K<sub>v</sub>1.2 voltage-gate potassium channel in open and closed state conformations. *J. Phys. Chem.* **2008**, *112*, 16966-16974.
- [5] Tombola, F.; Pathak, M.M.; Isacoff, E.Y. How Dose Voltage Open an Ion Channel? *Annu. Rev. Cell Dev. Biol.* **2006**, *22*, 23-52.
- [6] Chakrapani, S.; Cuello, L. G.; Cortes, D. M.; Perozo, E. Structural dynamics of an isolated-voltage sensor domain in lipid bilayer. *Structure* **2008**, *16*, 398-409.
- [7] Shafir, Y.; Durell, S. R.; Guy, H. R. Models of voltage-dependent conformational changes in NaChBac channels. *Biophys. J.* **2008**, *95*, 3663-3676.
- [8] Chakrapani, S.; Sompompisut, P.; Intharathep, P.; Roux, B.; Perozo, E. The activated state of a sodium channel voltage sensor in a membrane environment. *Proc. Natl. Acad. Sci. USA* **2010**, *107*, 5435-5440.
- [9] Jiang, Y.; Lee, A.; Chen, J.; Ruta, V.; Cadene, M.; Chait, B. T.; MacKinnon, R. X-ray structure of a voltage-dependent K<sup>+</sup> channel. *Nature* **2003**, *423*, 33-41.
- [10] Long, S. B.; Tao, X.; Campbell, E. B.; MacKinnon, R. Atomic structure of a voltage-dependent K<sup>+</sup> channel in a lipid membrane-like environment. *Nature* **2007**, *450*, 376-382.
- [11] Payandeh, J.; Scheuer, T.; Zheng, N.; Catterall, W.A. The crystal structure of a voltage-gated sodium channel. *Nature* **2011**, *475*, 353-358.
- [12] Baker, N.; MacCammon, J. A.; Holst, M. Adaptive Poisson-Boltzmann solver. <http://www.poissonboltzmann.org>
- [13] The theoretical and computational biophysics group; University of Illinois at Urbana-Champaign. Visual Molecular Dynamics. <http://www.ks.uiuc.edu/Research/vmd>
- [14] Grabe, M.; Lecar, H.; Jan, N. Y.; Jan, Y.L. A quantitative assessment of models for voltage-dependent gating of ion channels. *Proc. Natl. Acad. Sci. USA* **2004**, *101*, 17640-17645.

### **VITAE**

Miss Wannaruedee Wannapukdee was born on February 26, 1987 in Roi – et, Thailand. She graduated with Bachelor’s Degree of Science, major in Chemistry from Faculty of Science, Khon Kaen University, in 2009. She then continued her graduate degree at the Department of Chemistry, Chulalongkorn University. During the time she was studying in the Master of Science program at the Department of Chemistry.

Her present address is 505 Moo 18, Tambon Rob - Muang, Amphoe Muang, Roi - et, Thailand, 45000, e – mail : wanruedee.w@hotmail.com.